NASA Contractor Report 156862

Determining Sea-Ice Boundaries and Ice Roughness Using GEOS-3 Altimeter Data

(NASA-CR-156862) DETERMINING SEA-ICE BOUNDARIES AND ICE ROUGHNESS USING GEOS-3 ALTIMETER DATA (Computer Sciences Corp., Wallops Island, Va.) 49 p HC A03/MF A01 CSCL 08L G3/43

N80-22758

Unclas 46853

R. E. Dwyer

and

R. H. Godin

March 1980

National Aeronautics and
Space Administration

Wallops Flight Center
Wallops Island, Virginia 23337
AC 804 824-3411

NASA Contractor Report 156862

Determining Sea-Ice Boundaries and Ice Roughness Using GEOS-3 Altimeter Data

R. E. Dwyer
Computer Sciences Corporation
Wallops Island, Virginia 23337

and

R. H. Godin
National Weather Service
NOAA National Meteorological Center
Washington, DC 20233

Prepared Under Contract No. NAS6-2947

NASA
National Aeronautics and
Space Administration

Wallops Flight Center
Wallops Island, Virginia 23337
AC 804 824-3411

TABLE OF CONTENTS

1.0 INTRODUCTION AND SUMMARY

The contrast in the backscattering properties of sea ice and the open water ocean surface is so great that altimetry has been proven to have a unique all-weather capability for accurately determining the location of the sea ice boundary. In the March through June 1979, time period, GEOS-3 ice edge and roughness information was provided to the Fleet Weather Facility*/Joint Ice Center. The data was taken mainly in the Bering Sea ice fields and totalled over 200 arcs of data. In comparing the altimeter results to existing data sources (satellite visual and IR) it was evident that GEOS-3 data provided an accuracy in discriminating the ice edge equal to the best of the operational data sources. In addition to complementing the Ice Center existing sources, GEOS-3 provided an all weather capability and thus, on many occasions provided ice edge information that would otherwise not have been available. The Ice Center rapidly incorporated GEOS-3 data in their operational analyses and it became part of the thrice per week Bering Sea Ice Product.

This document describes the GEOS-3 satellite and radar altimeter instrumentation, details the ice boundary discrimination technique utilized and presents an analyses of the GEOS-3 data with respect to satellite visual and IR imagery. A brief description of the GEOS-3 real-time data system is also given.

2.0 GEOS-3 SPACECRAFT AND ALTIMETER CHARACTERISTICS

2.1 Spacecraft

The primary instrumentation carried by the GEOS-3 spacecraft is a dual mode radar altimeter. The spacecraft (pictured in Figure 2-1) also carries a variety of precise satellite tracking instrumentation. These C-band, S-band, laser and Doppler tracking systems are operated in conjunction with a worldwide network of

---

* On October 1, 1979, organization name was changed to Naval Polar Oceanography Center.

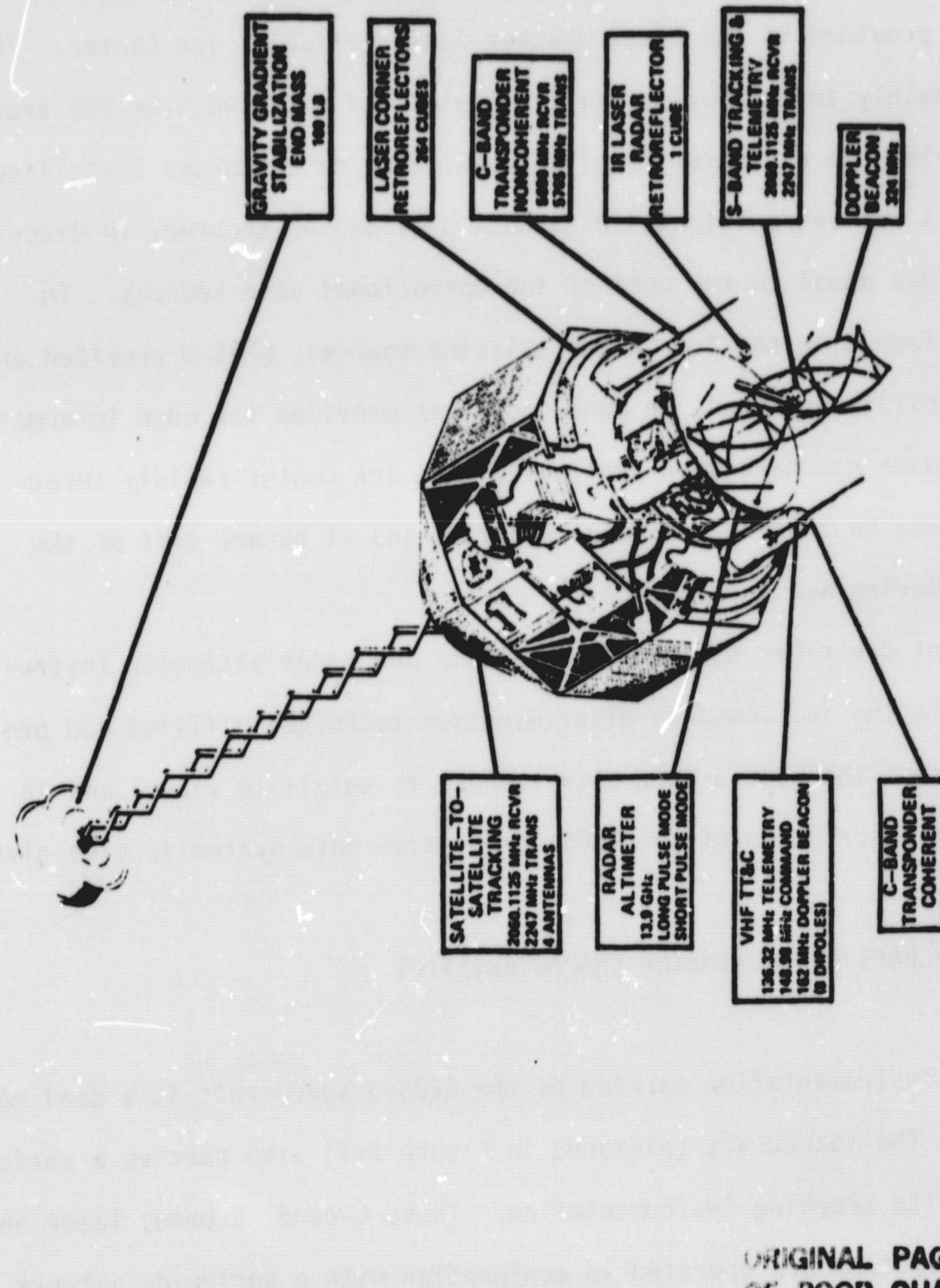

Figure 2-1. GEOS-3 Spacecraft (Cutaway View)

ORIGINAL PAGE IS OF POOR QUALITY

tracking stations to support various geodetic, gravimetric and tracking station calibration requirements. In addition, the precise tracking data is used to determine the orbit position from which the radar altimeter data is referenced.

The satellite was launched from the Air Force Western Test Range on April 9, 1975, into an 843 Km circular orbit with an inclination of 115 degrees to the earth's equator, and an orbital period of 101.8 minutes. The satellite weighs 340 Kg and measures 122 centimeters across the flats of the octahedronally shaped main body. The height of the main body is 131 centimeters measured from the top of the octahedronally shaped pyramid to the rim of the radar altimeter 61 centimeter parabolic antenna.

2.2 Radar Altimeter

The dual mode radar altimeter (Reference 1) operates at a frequency of 13.9 GHz. The global mode of the altimeter incorporates a pulse width of 200 nsec at a pulse repetition frequency of 100/sec and produces a range precision of 60 cm rms over a one second averaging period. The intensive mode of the altimeter utilizes an effective pulse width of 12.5 nsec, a repetition frequency of 100/sec, and produces a range precision over a one second averaging period of 20 cm rms. The effective 12.5 nsec intensive mode pulse width is implemented through pulse expansion and transmission of a linear FM modulated pulse with a duration of 1.2 μsec and then compression of the return energy at the same 100:1 ratio to produce a time domain return, equivalent to that which would be received from a 12.5 nsec transmitted pulse.

The altimeter transmits pulses of energy to the ocean surface and tracks the backscattered energy to precisely measure the distance between the satellite and ocean surface. In addition to the ranging function, the altimeter is instrumented with sampling gates to provide the pulse shape and amplitude of the

return energy. The precision range data is applied to fine grain ocean geoid determination and determining the location and magnitude of time dependent departures of the sea surface from the geoid as in the case of ocean current systems and ocean tides. Return pulse shape and amplitude data provides the means for sea-state (significant wave height) and wind speed estimation, determining water/ice boundaries, and other backscattering investigations.

3.0 ICE BOUNDARY DISCRIMINATION TECHNIQUES

3.1 Return Pulse Sampling Gates

Figure 3-1 illustrates the sampling gate timing and positioning for both the intensive and global mode of altimetry. Time T_0 represents the beginning of the return of the backscattered energy from the ocean surface. The altimeter range servo operates on the relative energy levels in the ramp (R) and plateau (P) gate regions to create error signals (ϵ = 2R-P) that drive the time opening of the ramp gate to the T_0 position. A digital representation of the time domain position of the gates (relative to the time of the transmitted pulse) is stored and then transmitted to ground telemetry receiving stations. Proper scaling of this transmitted "altitude" word provides the ranging or satellite altitude tracking function of the altimeter. The relative energy levels in all of the gates shown in Figure 3-1 are also telemetered to the ground stations and thus provide the return pulse shape and amplitude data used in determining the various oceanographic properties that can be remotely sensed by the altimeter. The relative gate positions are always as shown in Figure 3-1, that is, all gates move together in the time domain as the range servo operates to track the ocean return.

During the March through June 1979 sea ice activities conducted in conjunction with the Joint Ice Center, the GEOS-3 global mode altimeter was used

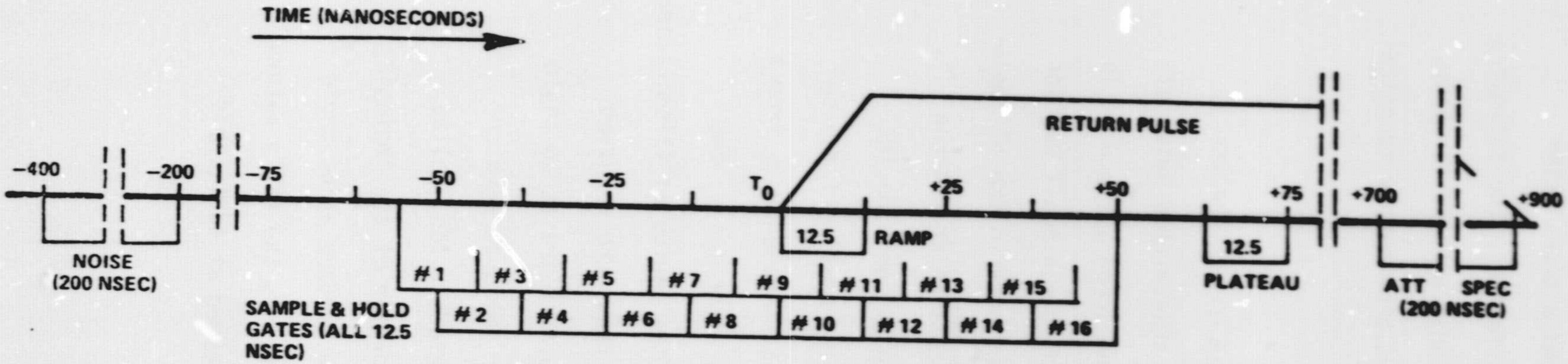

Intensive Mode Track

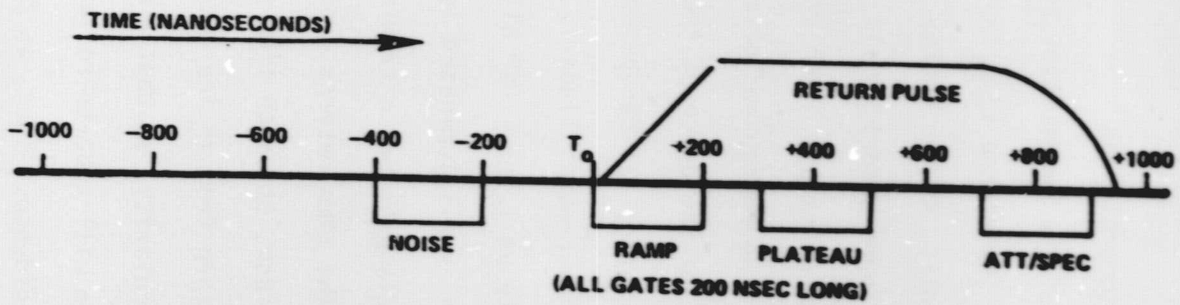

Global Mode Track

Figure 3-1. Sampling Gate Timing and Positioning

exclusively. The intensive mode of altimetry had experienced a transmitter failure in late 1978 after having far exceeded its design lifetime. The following data interpretation and analyses is, therefore, based on global mode performance. However, performance and analyses for the intensive mode would be nearly identical.

3.2 Data Analysis and Interpretation

Consider an example of the backscattering properties of smooth sea ice versus that of open water (Reference 2). In Figure 3-2, a transmitted pulse of width τ is directed at nadir. As the energy impinges on the ocean surface it is scattered (in the case of open water) in all directions and only a small portion of the total energy illuminating any given area is reflected back to the altimeter antenna. For open water, the energy reflected back to the altimeter antenna is not dependent on angle of incidence at the ocean surface but only on the instantaneous area illuminated. It can be seen, then, that from time $T = 0$ to $T = \tau$, the received power increases linearly as the area illuminated goes from a point at $T = 0$ to a circle at $T = \tau$. For all time periods after $T = \tau$, the geometry is such that the area illuminated is constant as the anulus of illumination spreads with increasing diameter but narrowing thickness, thus, the received power is constant until the time returns from the ocean surface are at an angle beyond the antenna beamwidth, at which time received power falls to zero.

Now consider the return from an ice covered ocean surface. Ice, unlike water, tends towards specularity, so that a much larger portion of the impinging energy at any given angle will tend to reflect off the ice surface at an angle equal to the angle of incidence. Thus, as shown in Figure 3-3, the early return (that received from nadir) is much stronger than that received at angles off nadir (i.e., the latter part of the return).

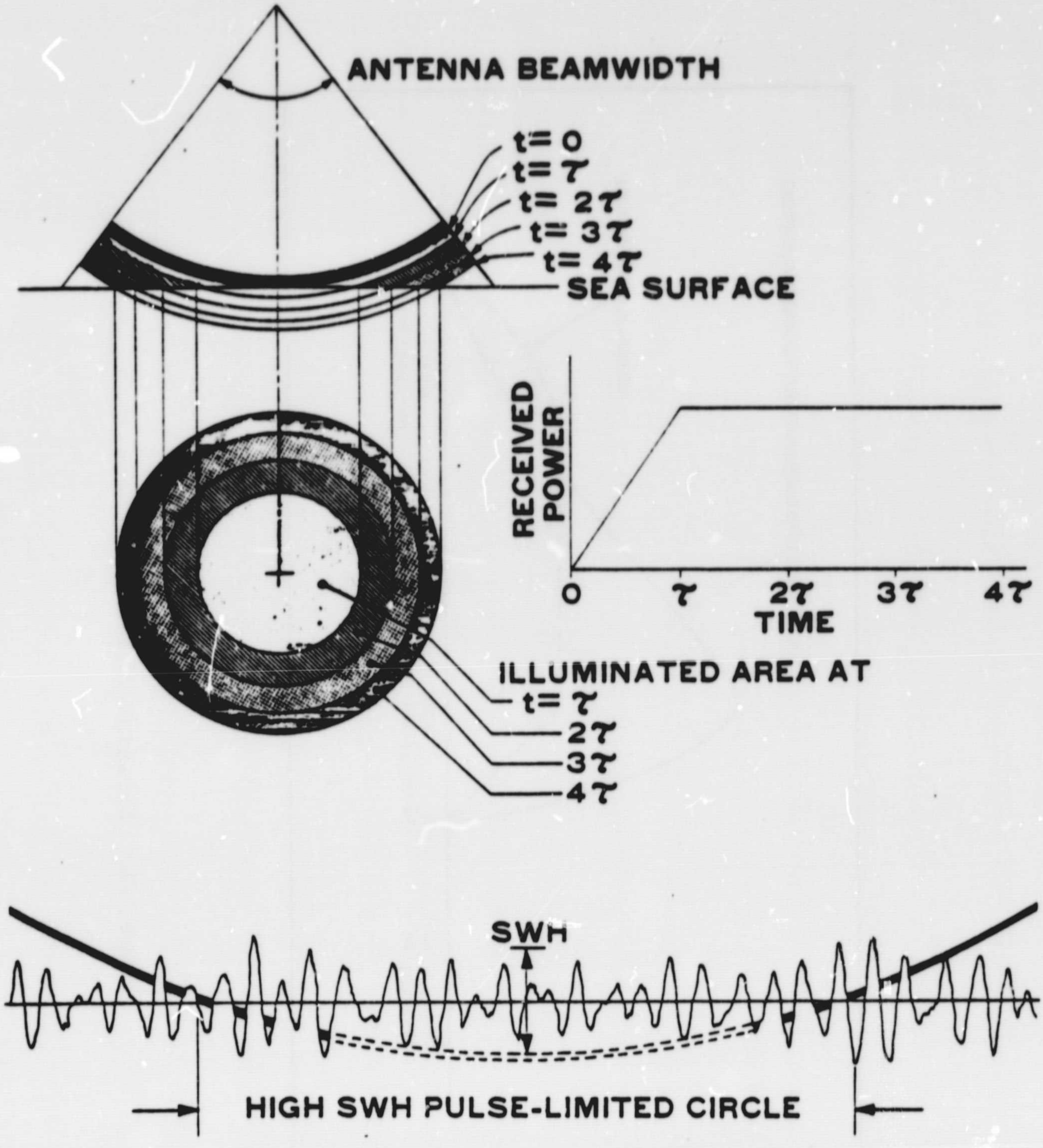

Figure 3-2. Backscattering from Ocean Surface

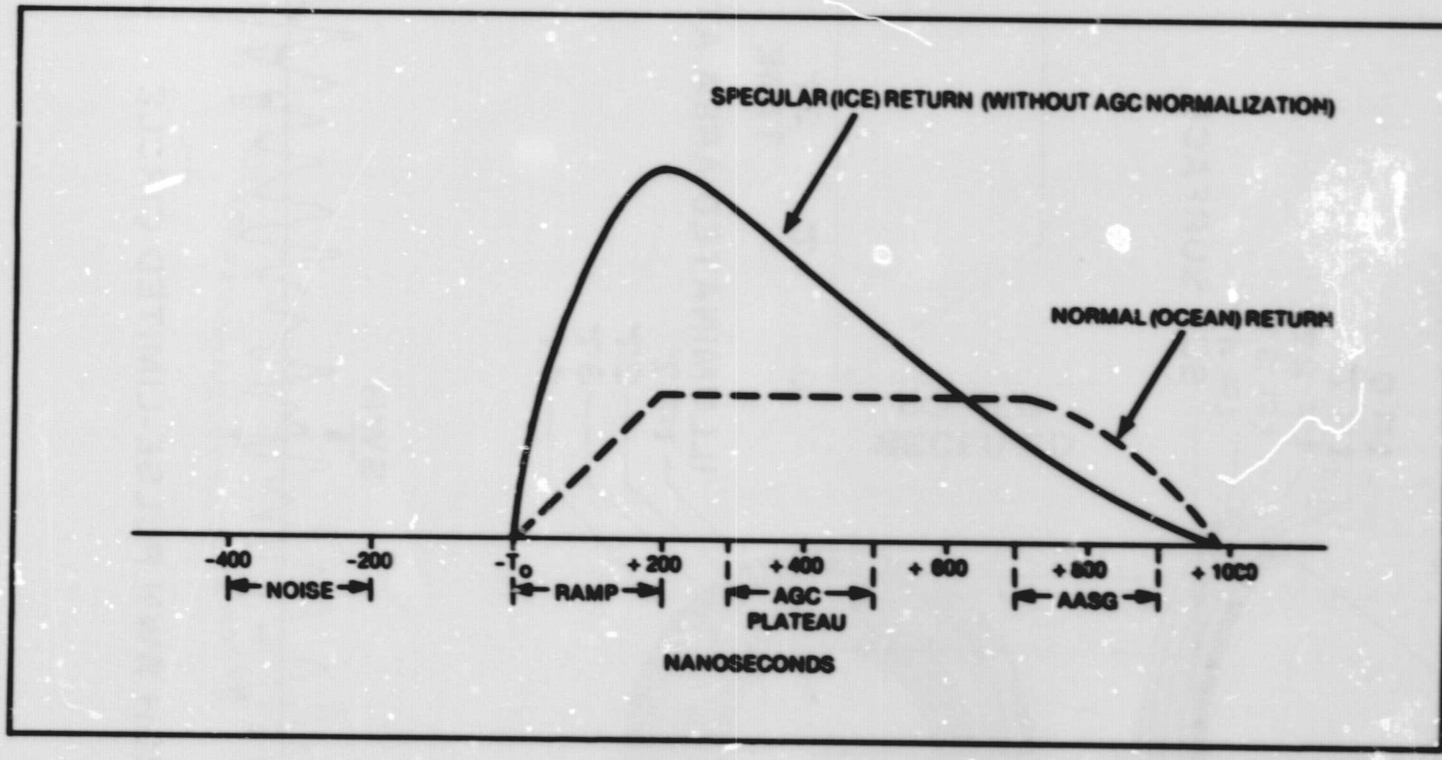

Figure 3-3. Ice and Ocean Return Waveforms

In using Figure 3-3 for descriptive purposes, license has been taken in displaying the specular (ice) return without the influence of the global tracker automatic gain control (AGC) normalization. In actuality, a non-AGC'ed waveform is not available from the altimeter. The global tracker AGC gate is positioned at the plateau gate location and functions to vary receiver gain to maintain the sampled plateau region at a constant level. A one second average of the AGC level is also telemetered to the ground and this AGC value is used as the measure of energy in the early (near nadir) part of the return. A one second average measure of energy received in the late return (i.e., from angles increasingly off nadir) is provided by the average attitude/ specular gate (AASG).

The above discussion suggests that a marked difference in AGC and AASG relative levels should be seen for ice backscattering versus water backscattering. To illustrate this, a GEOS-3 track (Figure 3-4) taken in the Bering Sea on March 16, 1979, is examined.

Figure 3-5 is a plot of the early (AGC) and late gate (AASG) relative energy levels for orbit 20319. The altimeter was turned on over ice, and remained on well past the ice edge. Note the drastic differences in the AGC and AASG signatures for the over ice and over water portions of this track. The dynamic changes from the ice to water medium are quite large and need only be calibrated to ground truth to distinguish at what point the ice edge was actually overflown.

In February 1979, the GEOS-3 Project worked with the Fleet Weather Facility/ Joint Ice Center to calibrate the altimeter discrimination to ground truth. The data signatures were found to be very repeatable at ice edges and rapidly an indexing algorithm was developed as shown and plotted in Figure 3-6. The index was calibrated to yield a value of zero at the ice edge.

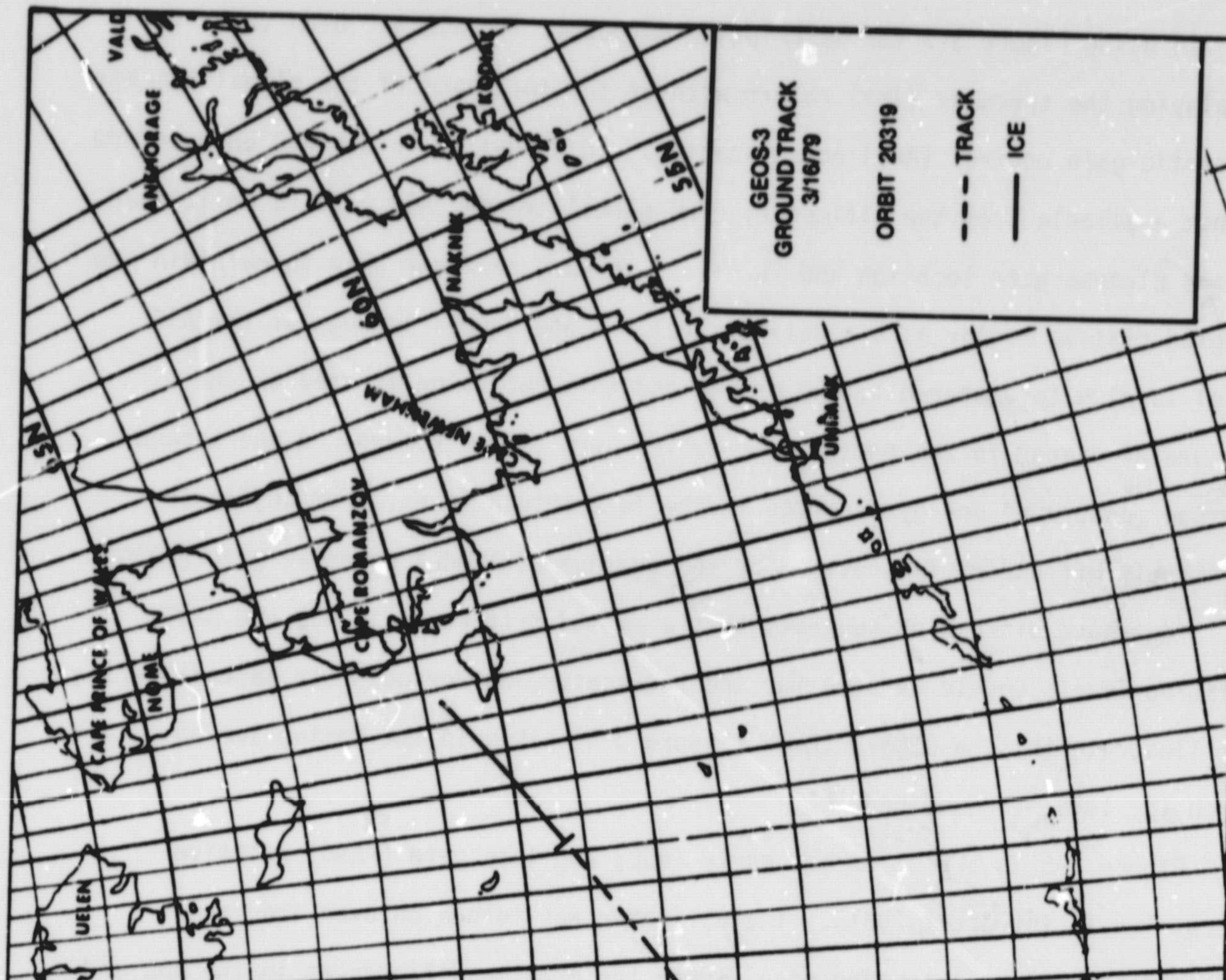
GEOS-3
GROUND TRACK
3/16/79
ORBIT 20319
TRACK
ICE
USSR
NAVARIN
UELEN
CAPE PRINCE OF WALES
NOME
CAPE ROMANZOV
CAPE NEWENHAM
NAKNEK
ANCHORAGE
KODIAK
UNIMAK
ADAK
60N
20319
175E
180
175W
170W
165W
160W

Figure 3-4

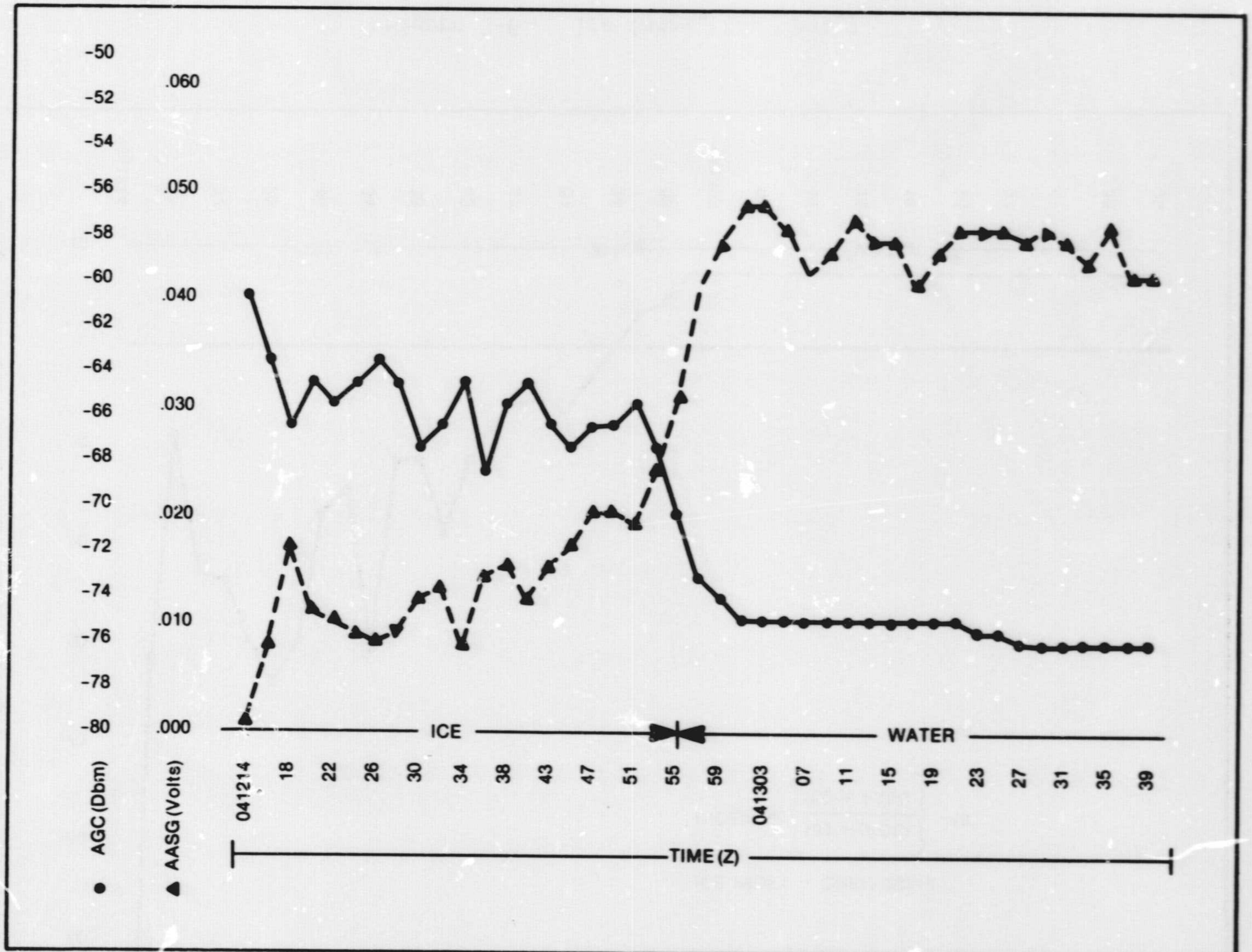

Figure 3-5. AGC and AASG vs. Time, Orbit 20319

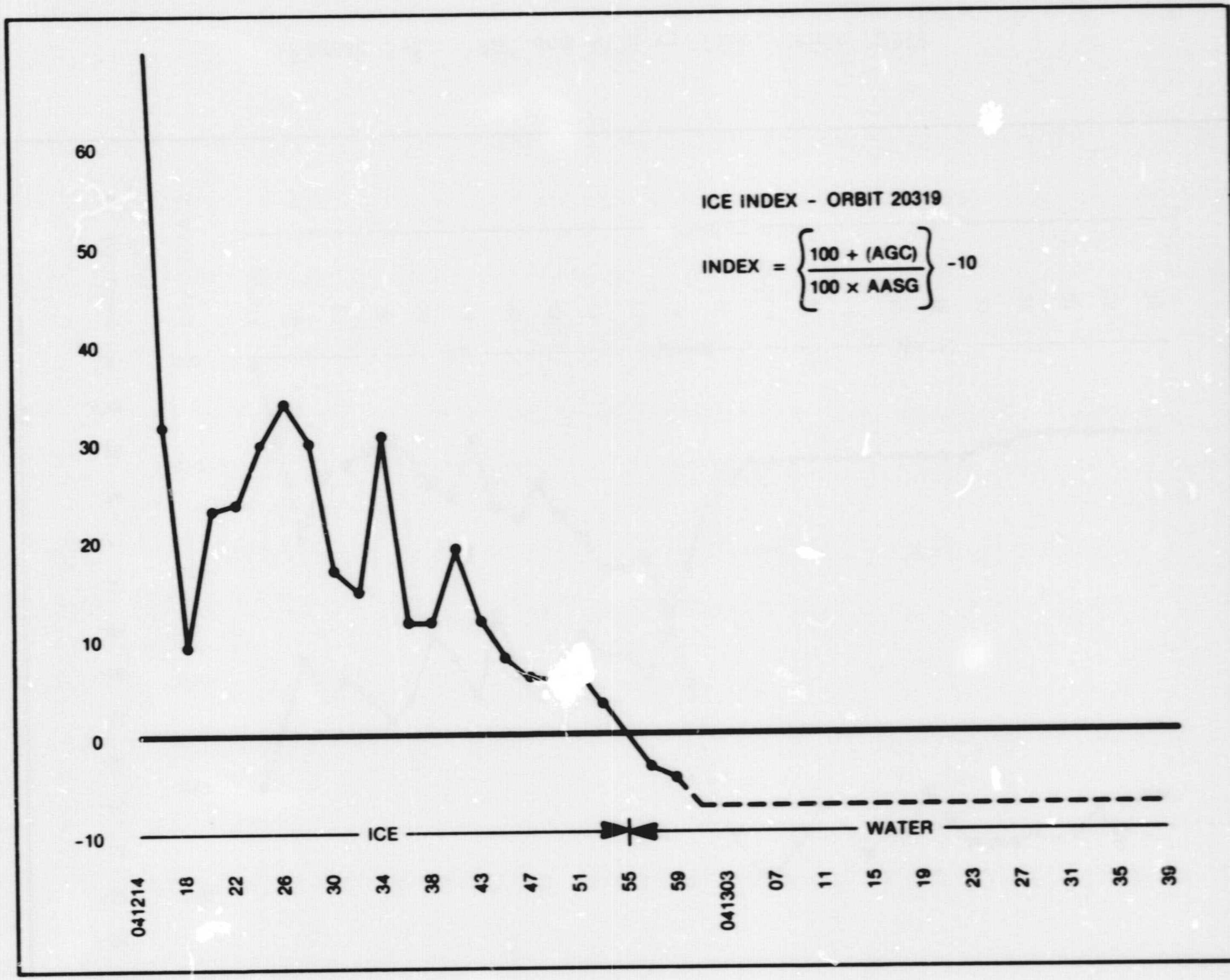

Figure 3-6. Ice Index, Rev. 20319

In addition to the ice edge discrimination at index value of zero, it is also apparent that the variations in the index values are caused by different ice characteristics. For instance very smooth ice would yield a high index resulting from a high level of energy in the early (AGC) gate and a very low level in the late (AASG) gate. Conversely, as the ice surface becomes more and more rough, energy would be diminished in the early gate due to more scattering at nadir, while energy in the late gate would increase due to there being more facets or small areas of ice lying normal to the off-nadir angles of incidence; thus causing a low value of ice index. Efforts are continuing at the Ice Center to quantize the ice roughness capabilities evident in the altimeter data.

In the March through June 1979, time period, the GEOS-3 calibrated ice index information was provided to the Ice Center via the GEOS-3 Near-Real-Time Ocean Products Processing and Communications System which will be briefly explained in Section 4.0 of this document. The data were taken mainly in the Bering Sea ice fields and totalled over 200 arcs of data. The ice files contained records of time, latitude, longitude, AGC and AASG values and the ice index at two second intervals along the GEOS-3 tracks. The Ice Center analysis of the GEOS-3 data in comparison to existing data sources (satellite visual and IR) are presented in Section 5.0.

4.0 GEOS-3 NEAR-REAL-TIME OCEAN PRODUCTS PROCESSING AND COMMUNICATIONS SYSTEM

4.1 General

The GEOS-3 near-real-time data system (Reference 3) is briefly described here in its application of providing data to a remote site (the Joint Ice Center) in a time frame commensurate with operational application. The system had been operational since March 1, 1978, and had been implemented to provide GEOS-3 altimeter sea state (significant wave height, Reference 4), wind speed (Reference 5), and Gulf Stream current boundary and velocity data (Reference 6), to various users. The main users were NOAA facilities located in Maryland, Florida, Washington State, California, Colorado, Alaska and Hawaii. With the failure of the intensive mode altimeter transmitter in September 1978, sea state and Gulf Stream information were no longer available in the system. Wind speed estimates continued to be provided and in February 1979, program modifications were implemented to establish the flow of ice boundary and roughness (ice index) data. On July 1, 1979, with the completion of the Northern Hemisphere ice season (below 65° North latitude) the data system and NASA activities using the GEOS-3 altimeter were terminated.

4.2 Data Flow and Processing

The data flow of the near-real-time data system is illustrated in Figure 4-1. Raw GEOS-3 altimeter data was acquired at the 13 locations of the NASA Space Tracking and Data Network or via data relay through the geosynchronous ATS-6 satellite. The worldwide coverage afforded by these sources is illustrated in Figure 4-2. The data were transmitted by NASA Communications facilities in real-time to the GEOS-3 Control Center at NASA Goddard Space Flight Center in Greenbelt, Maryland.

At GEOS-3 Control, that portion of the total telemetry data needed for significant wave height ($H_{1/3}$), wind speed, ice boundary, and current boundary

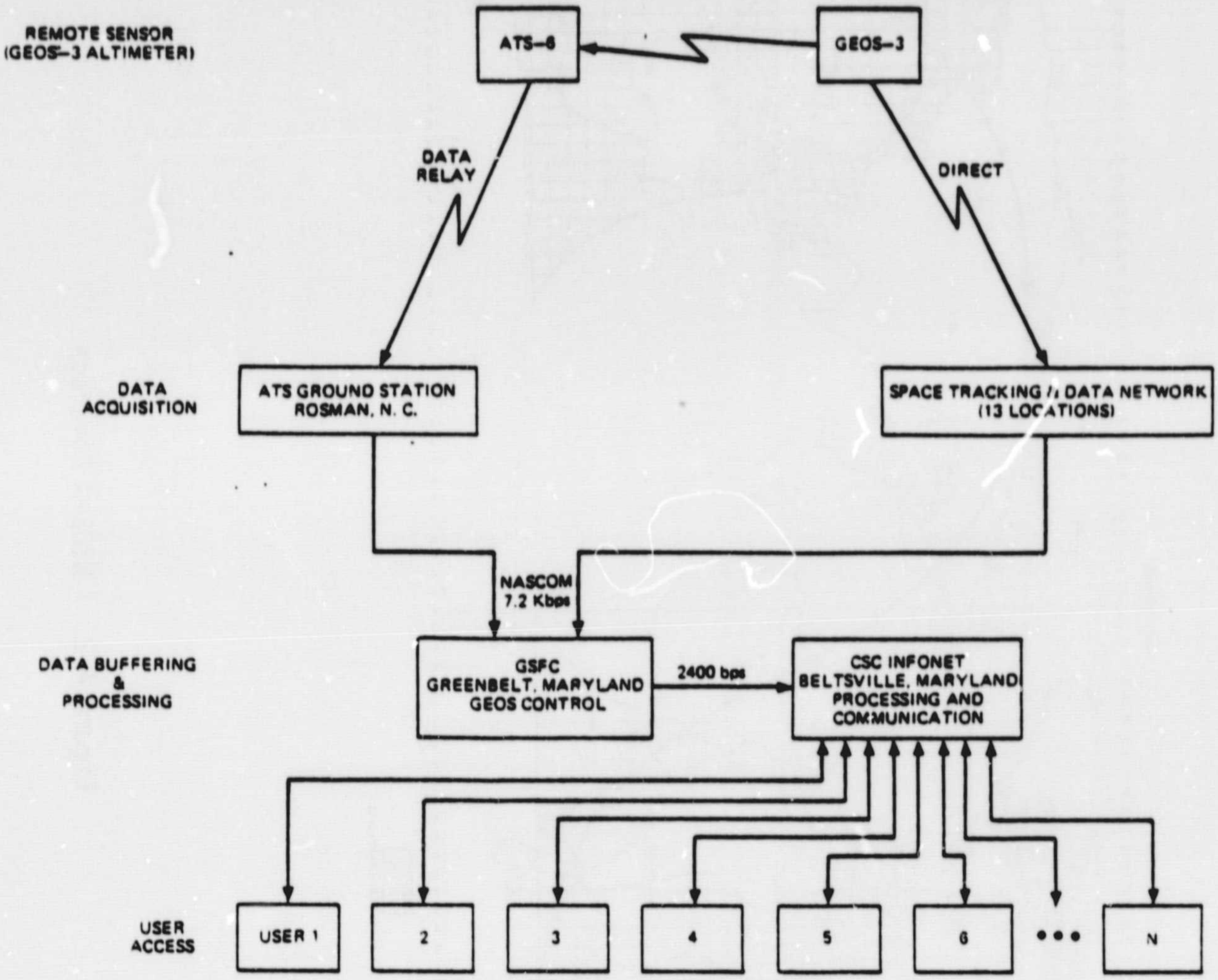

Figure 4-1. GEOS-3 Near-Real-Time System Data Flow

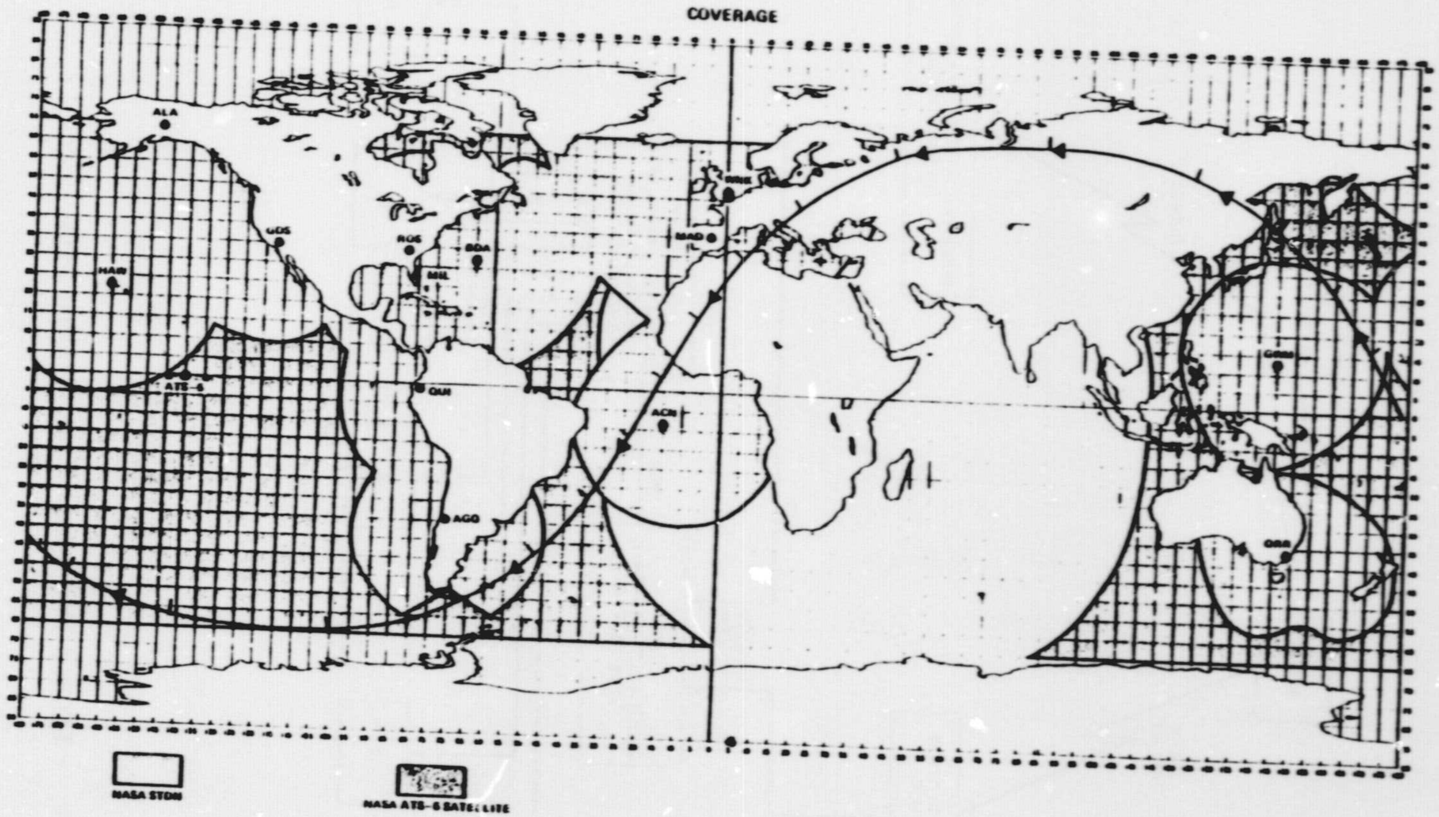

Figure 4-2. GEOS-3 Coverage

determination was buffered to magnetic tape. This operation was also accomplished in real-time.

Immediately after the real-time data acquisition was complete, the buffered data accumulated on magnetic tape was transmitted by high speed communications to the Computer Sciences Corporation INFONET Center in Beltsville, Maryland. The data was processed at the INFONET Center into GEOS-3 oceanic products and files of data were made available for access by the user community. User access was on a call-up basis by means of user-supplied terminals such as the widely used and economically available ASCII character set interactive printer terminals.

Data was made available for user access within approximately 15 minutes of the real-time data acquisition. At least three days of data remained in the system for access prior to its being dumped to magnetic tape for archival purposes.

The ice file was created by processing each logical record of GEOS-3 altimeter data (i.e., each two second major frame of telemetry) and evaluating the AASG (late gate) for a predetermined threshold value. As can be seen in Figure 3-5, AASG is consistently more than .045 volts with the spacecraft over water. The AASG threshold was set at .033 volts and any frame of data with a value AASG $\leq$ .033 volts created a record in the ice file. With a reduced return in the AASG (late gate), altimeter backscattered energy from off nadir is diminished indicating a specular return and the possibility of ice. (Conversely, as can be seen in Figure 3-5, AGC increases indicating a strong return from nadir.) Other possibilities could be land, which also causes a specular return, and, of course, ice on land masses. Ambiguities as to whether the returns are from sea-ice or land are resolved by calculating satellite ground track latitude/longitude positions.

An ice file is shown in Figure 4-3 for orbit 20319 taken on March 16, 1979. Time is in HHMMSS GMT, TCG is the spacecraft major frame counter, and latitude/longitude points are in the geodetic coordinate system. AASG is in volts, AGC is in dbm, and the ice index is calculated as follows:

$$\text{INDEX} = \left[\frac{100 + \text{AGC}}{100 \cdot \text{AASG}}\right] \quad -10$$

It should be noted that the index numbers shown cannot be reconstructed precisely since, for the user record, the index value is truncated at whole numbers and AASG and AGC are truncated at the third decimal place.

For completeness, Figure 4-4 shows the accompanying surface wind file for orbit 20319. Note that the $H_{1/3}$ (significant wave height) column is blank since the intensive mode of altimetry was not operating. The wind values are in meters per second. The five values in each record are evenly distributed between the record latitude/longitude points with the first wind value in each record agreeing with the record lat/long point*[1]. The wind speed can be seen to vary between approximately 12 to 15 meters/sec as GEOS-3 comes off the ice edge and then diminish to approximately 3 meters/sec as GEOS-3 traverses further South over the Pacific Ocean.

---

*[1] The value after the slash (e.g., 13.3/3) is in the range one through three and is a data quality indicator for the wind speed estimate. It represents the number of contiguous frames of data that were averaged to produce the wind speed estimates. The maximum value of three indicates the best data quality.

ICE FILE - 20319 79/03/16

TIME	TCG	LAT.	LONG.	AASG	AGC	INDEX
41214	6059218	60.62	-167.51	.001	-60.935	269
41216	6059219	60.56	-167.72	.008	-63.611	32
41218	6059220	60.49	-167.93	.017	-66.484	9
41220	6059221	60.43	-168.14	.011	-64.647	23
41222	6059222	60.37	-168.35	.010	-65.463	24
41224	6059223	60.31	-168.56	.009	-64.181	30
41226	6059224	60.25	-168.77	.008	-63.676	34
41228	6059225	60.19	-168.98	.009	-64.609	30
41230	6059226	60.12	-169.19	.012	-67.405	17
41232	6059227	60.06	-169.39	.013	-66.914	15
41234	6059228	60.00	-169.60	.008	-64.609	31
41236	6059229	59.93	-169.80	.014	-68.387	12
41238	6059230	59.87	-170.01	.015	-65.140	12
41240	6059231	59.80	-170.21	.012	-64.207	19
41243	6059232	59.71	-170.51	.015	-66.422	12
41245	6059233	59.64	-170.71	.017	-67.171	8
41247	6059234	59.58	-170.92	.020	-66.631	6
41249	6059235	59.51	-171.12	.020	-66.254	6
41251	6059236	59.45	-171.31	.019	-65.878	7
41253	6059237	59.38	-171.51	.024	-67.073	3
41255	6059238	59.31	-171.71	.031	-70.007	0
41257	6059239	59.25	-171.91	.041	-73.781	-3
41259	6059240	59.18	-172.10	.045	-74.942	-4

```
!CHANGE ICE I20319
!CAT I20319
I20319-PNC/LIB$
!DROP SSBURR
!OFF
USAGE ON 03/15/79 AT 23:53:40
SRU'S:18.8       ELAPSED TIME: 00:03:56
GOOD BYE.
```

Figure 4-3. Ice File, Orbit 20319

```
>?~wxE
PORT: 79
CENTER: NN
SUBS:  GPS
[illegible]
03/15/79 23:49:44-00 107-20-02-079-2000
!DO SSTATE
 ** SEA STATE PROGRAM - VERSION 7902-6 ***
 SPECIAL PROCESSING DESIRED?N

*** GLOBAL MODE DATA - NO H-1/3 WILL BE COMPUTED

*** ICE FILE WILL BE CREATED
*** SUMMARY FILE CREATED: A20319
 STOP
SRU'S:11.7
GPS362   O8-PNC/LIB$ 57355 3017501376
 END OF RUN
!LIST A20319
 GEOC 20319 79/03/16  ASCTIM  75  3 42  8      ASCLON   324.64
  TIME     LAT      LONG    H1/3   GAM ************ W I N D S ************
  413 1   59.06 -171.94      *          11.7/2 11.9/3 12.1/3 12.5/3 12.9/3
  41321   58.38 -173.87                 13.3/3 13.4/3 14.2/3 14.9/3 15.1/3
  41342   57.63 -175.82                 15.2/3 15.5/3 15.3/3 15.2/3 15.6/3
  414 2   56.90 -177.61                 15.8/3 16.1/3 15.8/3 15.9/3 15.4/3
  41423   56.10 -179.42                 15.5/3 15.9/3 15.5/3 15.4/3 15.2/3
  41443   55.32  178.92                 14.6/3 14.2/3 13.7/3 13.2/3 12.8/3
  415 4   54.48  177.25                 12.5/3 12.3/3 12.3/3 12.3/3 12.1/3
  41524   53.66  175.72                 12.1/3 11.5/3 10.9/3 11.0/3 10.8/3
  41545   52.78  174.17                 10.4/3  9.6/3  9.3/3  7.3/3  6.4/3
  416 5   51.93  172.75                  7.2/3  7.9/3  7.3/3  6.9/3  6.8/3
  41626   51.02  171.32                  6.8/3  5.8/3  5.5/3  6.8/3  6.4/3
  41646   50.14  169.99                  6.2/3  5.4/3  4.5/3  3.8/3  3.3/3
  417 7   49.20  168.66                  2.8/3  3.2/3  3.5/3  3.4/3  2.9/3
!LIST ICE
```

Figure 4-4.   Surface Wind File, Orbit 20319

Figure 4-5 illustrates the typical coverage in the Bering Sea provided by GEOS-3 over a sixteen day period (March 1-16, 1979). The figure illustrates the portions of the GEOS-3 subsatellite tracks which overflew ice. It should be noted that about twice as many tracks (i.e., 4 tracks per day) in the Bering Sea area are possible but only those shown actually achieved data due to priority conflicts for telemetry ground station support. GEOS-3 has no data storage capability, therefore, each data acquisition required real-time station support.

5.0 DATA ANALYSIS

5.1 General

The GEOS-3 radar altimeter data was compared with satellite imagery which is routinely available at the Joint Ice Center. The availability of mostly cloud free satellite imagery was the prime criteria for the selection of the case studies. The primary sensors and imagery utilized in the analysis are described as follows.

Defense Meteorological Satellite Program (DMSP), Reference 7. The visible (HR) and thermal infrared (MI) channel imagery were in the form of positive transparencies. HR and MI data are geometrically coherent at the sensor, and have a two nautical mile resolution. The HR channel detector has a peak response at 0.8 micrometers (μm) and a spectral interval of 0.4 - 1.1 μm. The processed film density is linearly proportional to scene reflectivity.

The MI channel detector has a flat response from 8 μm to 13 μm. Electronic shaping of the detector output in the sensor results in a linearly increasing function of scene black body temperature over the range of 210°k to 310°k.

National Oceanic and Atmospheric Administration (NOAA) TIROS-N, Reference 8. The Advanced High Resolution Radiometer (AVHRR), High Resolution Picture Transmission (HRPT) imagery were in the form of photograph quality hardcopies. The visible/near IR (Channel 1) and infrared (Channel 4) imagery

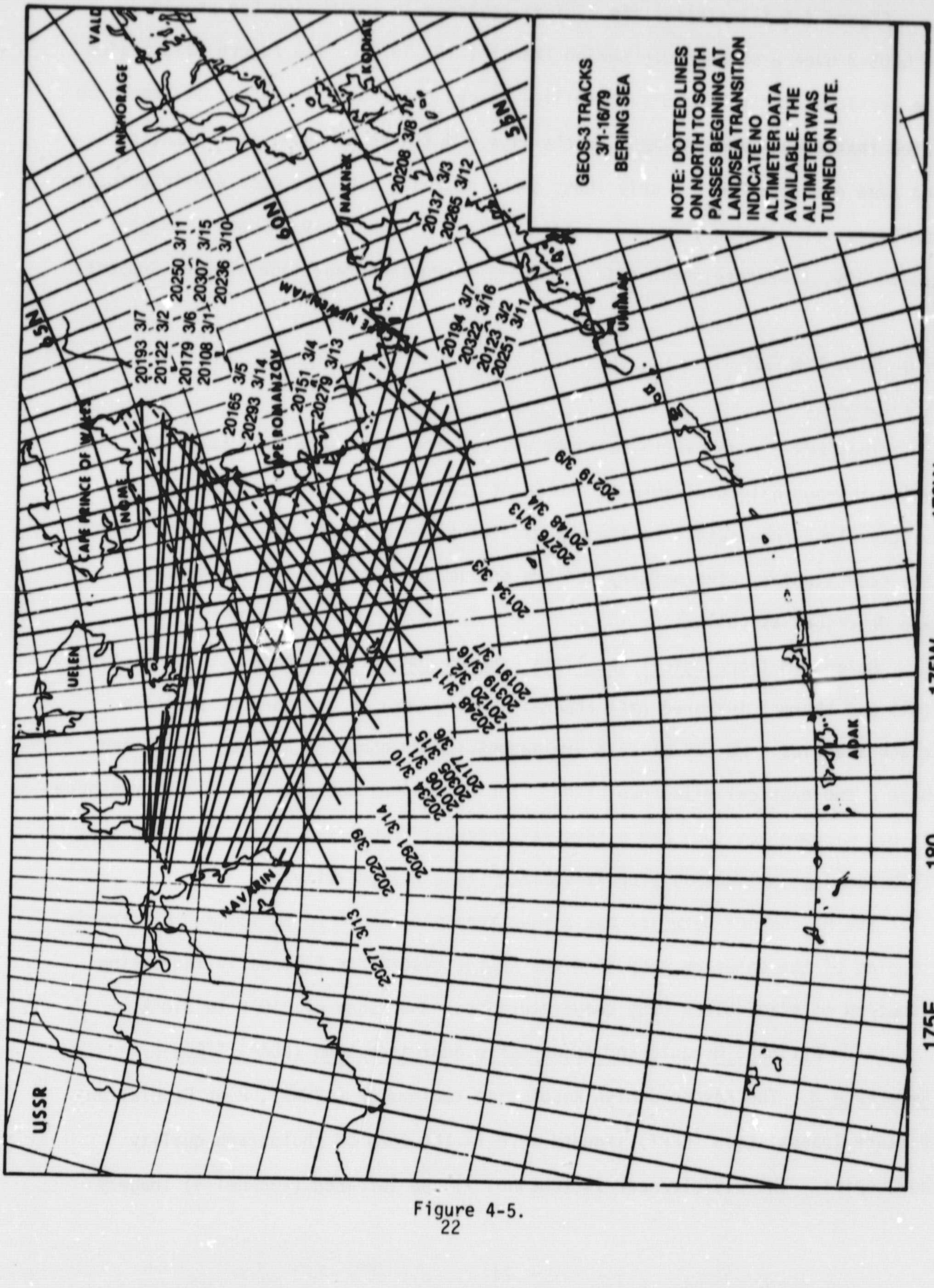
GEOS-3 TRACKS
3/1-16/79
BERING SEA
NOTE: DOTTED LINES ON NORTH TO SOUTH PASSES BEGINING AT LAND/SEA TRANSITION INDICATE NO ALTIMETER DATA AVAILABLE. THE ALTIMETER WAS TURNED ON LATE.
USSR
UELEN
NOME
CAPE PRINCE OF WALES
ANCHORAGE
KODIAK
NAKNEK
CAPE ROMANZOV
NAVARIN
UNIMAK
ADAK
65N
60N
55N
160W
165W
170W
175W
180
175E
20193 3/7
20122 3/2
20179 3/6
20108 3/1
20250 3/11
20307 3/15
20236 3/10
20165 3/5
20293 3/14
20151 3/4
20279 3/13
20208 3/8
20137 3/3
20265 3/12
20194 3/7
20322 3/16
20123 3/2
20251 3/11
20219 3/9
20276 3/13
20148 3/4
20134 3/3
20191 3/7
20319 3/16
20120 3/2
20248 3/11
20177 3/6
20305 3/15
20106 3/1
20234 3/10
20291 3/14
20220 3/9
20277 3/13

Figure 4-5.

have a 1.1 km resolution. The visible/near IR channel 1, has a wavelength of 0.55 μm to 0.90 μm. The infrared channel 4, has a wavelength of 10.5 μm to 11.5 μm.

Table 5-1 contains the legend for Figures 5-3, 5-5, and 5-7 of the case studies.

TABLE 5-1

GEOS-3 Track Legend

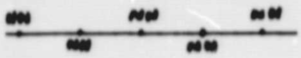	Portions of track with positive index values
	Portions of track with negative index or water signature.
m	Missing Data Point

ICE Analysis Legend

7-8	=	7-8 octas of ice cover
O/W	=	open water, less than 1 octa* of ice cover
YNG	=	young ice, 10 to 30 cm thick
FY	=	first year ice, 30 to 200 cm thick
N	=	new ice
———	=	ice boundary
— —	=	estimated ice boundary
ICE FREE	=	no sea ice present
	=	fast ice

5.2 Case Study of 02-03 March 1979 (Figs. 5-1, 5-2, 5-3)

Track 20120

TIROS-N visible imagery (Fig. 5-1) shows very good agreement in the location of the ice edge along the southern portion of track 20120 (Fig. 5 -3).

*Note: Octa is a commonly used term in ice analysis meaning "eighths".

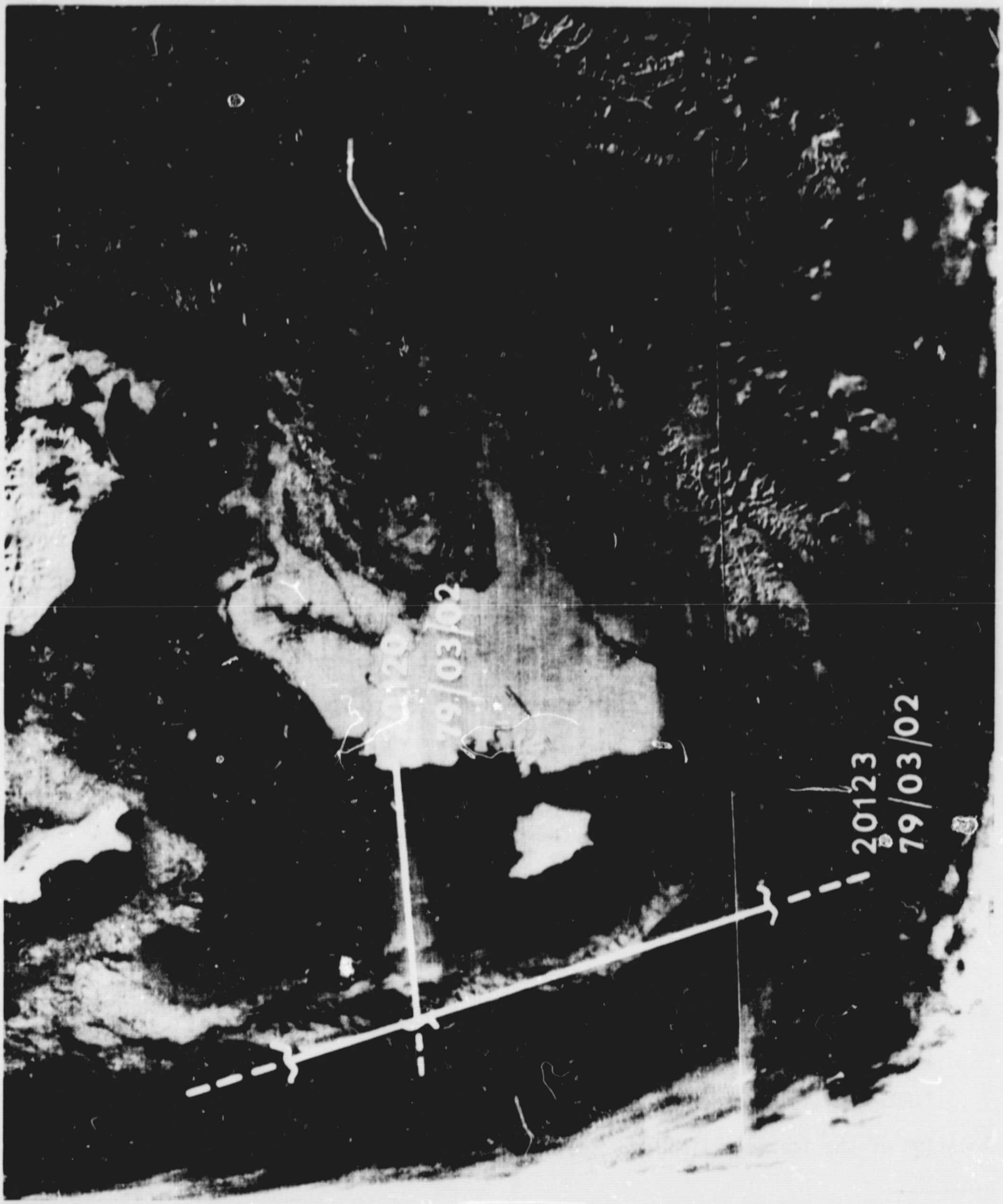

Fig. 5-1. TIROS-N Visual Satellite Observation, 0031 GMT March 02, 1979, with GEOS-3 Tracks 20120 and 20123

Fig. 5-2. DMSP Visual HR Channel Satellite Observation, About 2200 GMT, March 2, 1979, with GEOS-3 Track 20137

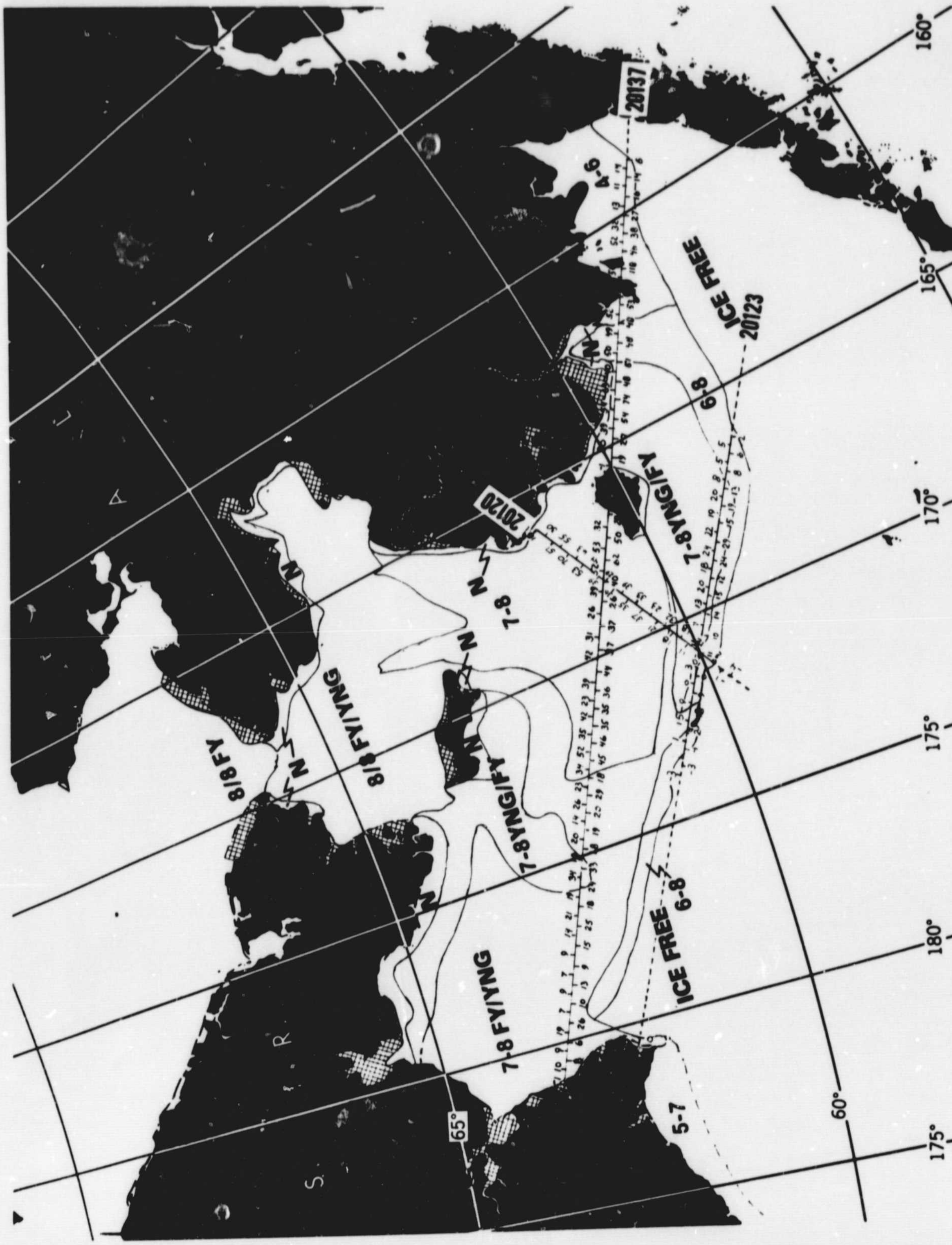

Fig. 5-3. Sea Ice Analysis March 2-3, 1979; With GEOS-3 Track 20120, 0239 GMT March 2, 1979; Track 20123, 0735 GMT March 2, 1979; Track 20137, 0721 GMT March 3, 1979.

Low index values along the track in the 2 to 11 range were observed within the 6-8 octas concentration boundary prior to exiting the ice zone.

Track 20123

Three ice edges were detected along track 20123 in the vicinity of 166°W, 174°W, and 10 nautical miles from the coast of the Soviet Union. Indexes with values of 0 were observed east of St. Matthew Island. These values correlate well with some large water openings observed in the TIROS-N imagery (Fig. 5-1).

There was a five hour time difference between the transits of tracks 20120 and 20123. A consistency of indexing was noted at the intersection of the two tracks where index values of 10 and 11 were observed.

Track 20137

One of the more striking features of both TIROS-N (Fig. 5-1) and DMSP imagery (Fig. 5-2) is the increased reflectivity of the ice drifting southward past the East coast of St. Lawrence Island. The increase of reflectivity or whiter shades depicted in the imagery are sensed by the altimeter as lower index values (14-29) between 173W and 175W, as compared to index values in the 30 to 50 range East of 173W for the region of smooth young ice. The whiter shades of the mostly first year ice West of 176W are sensed with index values in the 6-19 range.

5.3 Case Study of 26-27 March 1979 (Figs. 5-4, 5-5)

Track 20478

The TIROS-N visible imagery (Fig. 5-4) detected open water areas near the Alaskan Coast and to the south of St. Lawrence Island. Along the eastern portion of GEOS track 20478 a missing index value falls within the analyzed open water area (Fig. 5-5). To the south of St. Lawrence Island four negative index values in the -1 to -2 range fall within the analyzed open

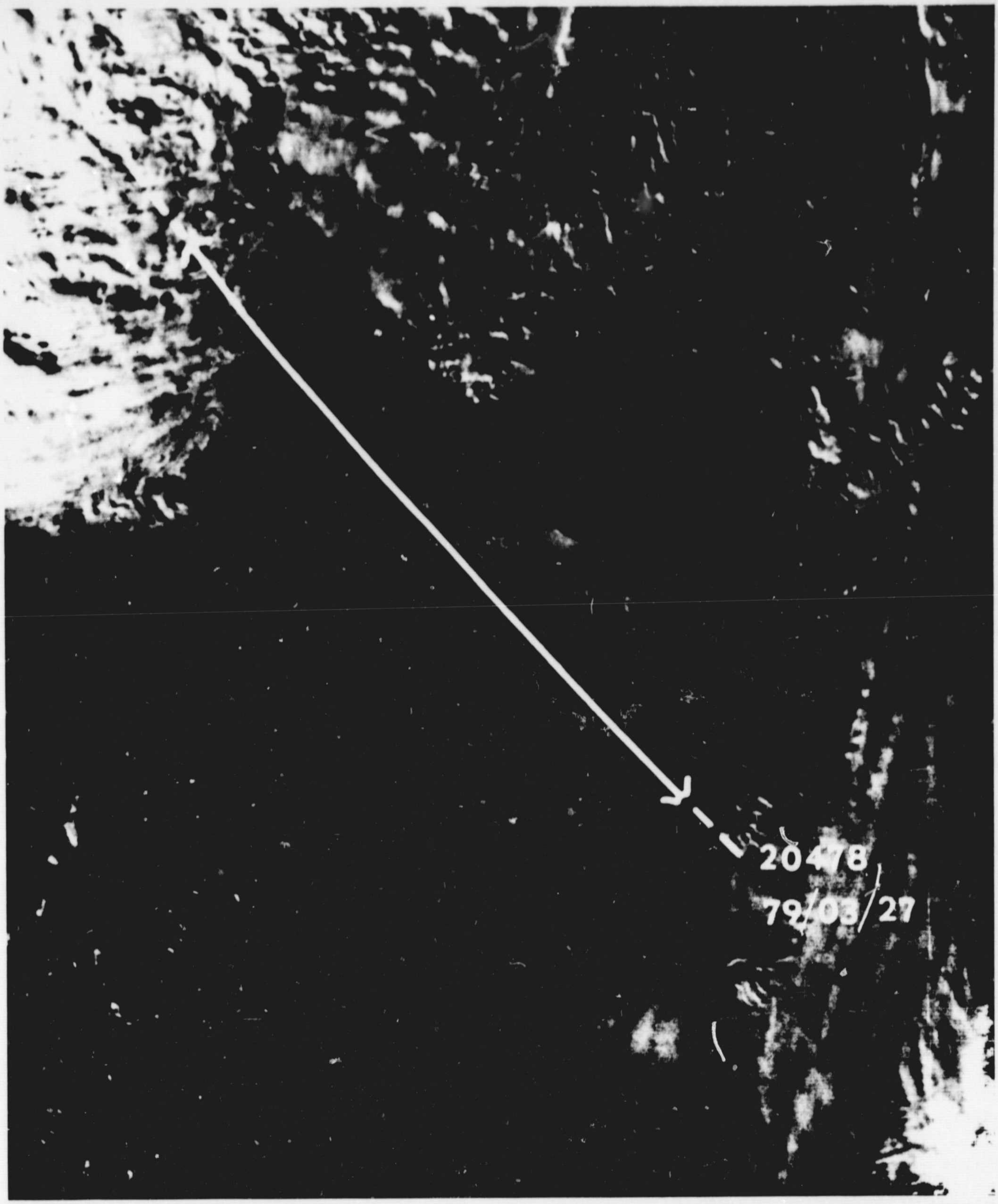

Fig. 5-4. TIROS-N Visual Satellite Observation, 0124 GMT March 26, 1979, with GEOS-3 Track 20478.

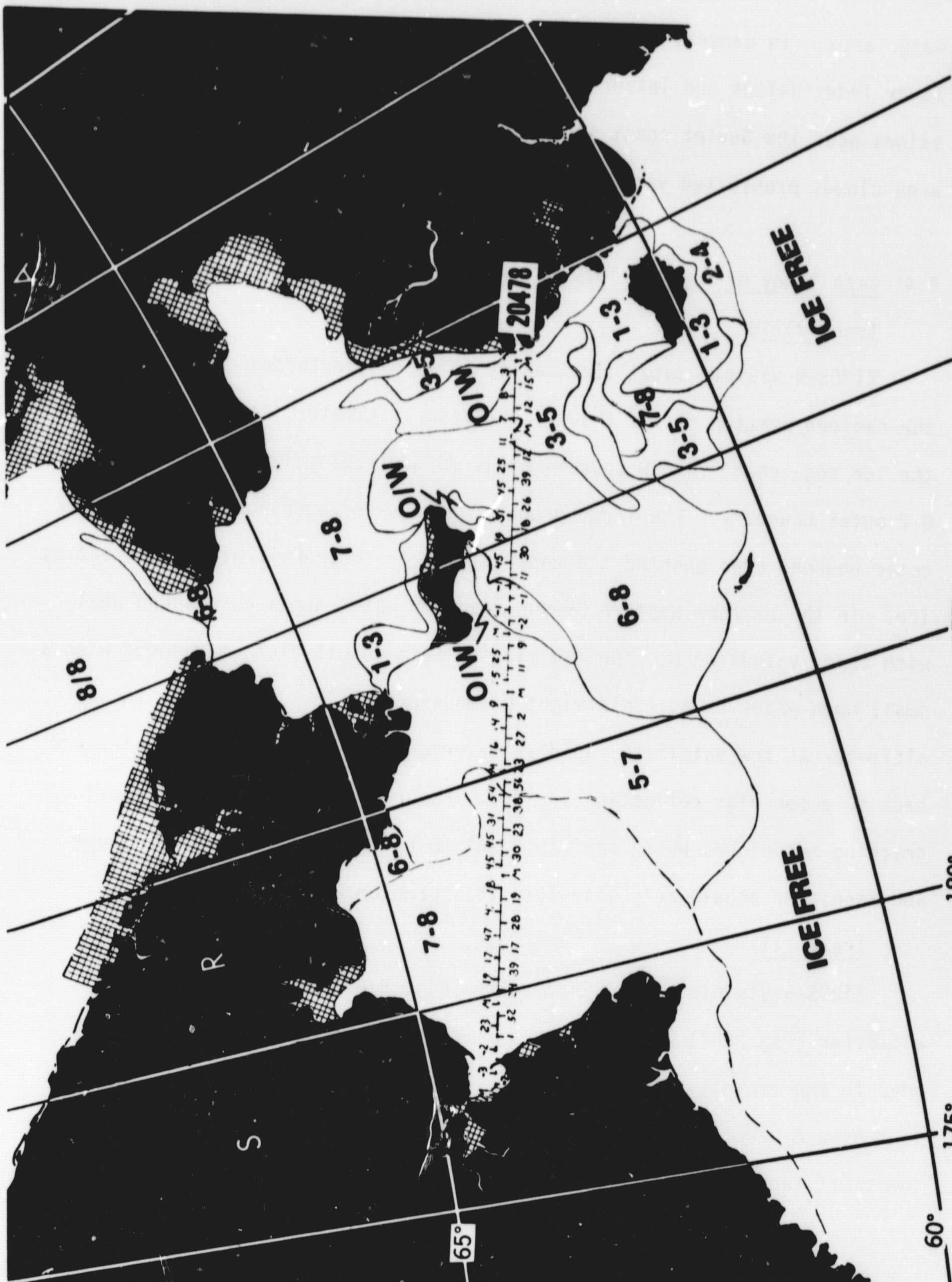

Fig. 5-5. Sea Ice Analysis March 26, 1979, with GEOS-3 Track 20478, 0945 GMT March 27, 1979

water area. In general there is a direct relationship observed between lower index values and lesser concentrations of ice. The negative index values near the Soviet coast imply open water conditions, however, in this area clouds prohibited verification.

5.4 Case Study of May 11, 1979 (Figs. 5-6, 5-7)

Track 21118

TIROS-N visible satellite imagery (Fig. 5-6) detected cloudiness along the eastern portion of the track. The radar altimeter (Fig. 5-7) detected the ice edge near 174.6°W approximately 30 nautical miles within the analyzed 0-2 octas boundary. The large proportion of water openings within the 0-2 octas bounded area enabled the radar altimeter to transit without detecting ice. In the extreme Western Bering Sea, open water areas correspond well with index values of 0. The two missing data points also correspond with a small open water area. This might be caused by a loss of lock in the altimeter as the satellite rapidly traverses from a specular, to water and back to a specular reflecting surface. Future altimeter design employing tracking techniques which rapidly adapt to varying return waveform shape and magnitude should help alleviate this problem.

Track 2117

TIROS-N visible satellite imagery (Fig. 5-6) and the GEOS-3 radar altimeter (Fig. 5-7) were both in agreement in the detection of the ice edge in the vicinity of 169°W. The open water area between 176°W and 180° is sensed by the altimeter with index values of -3 and -4 as the satellite comes off land into the open water.

5.5 Summary

From the case studies presented in this report and other experimental/

Fig. 5-6. TIROS-N Visual Satellite Observation, 0147 GMT
May 11, 1979, with GEOS-3 Tracks 21117 and 21118.

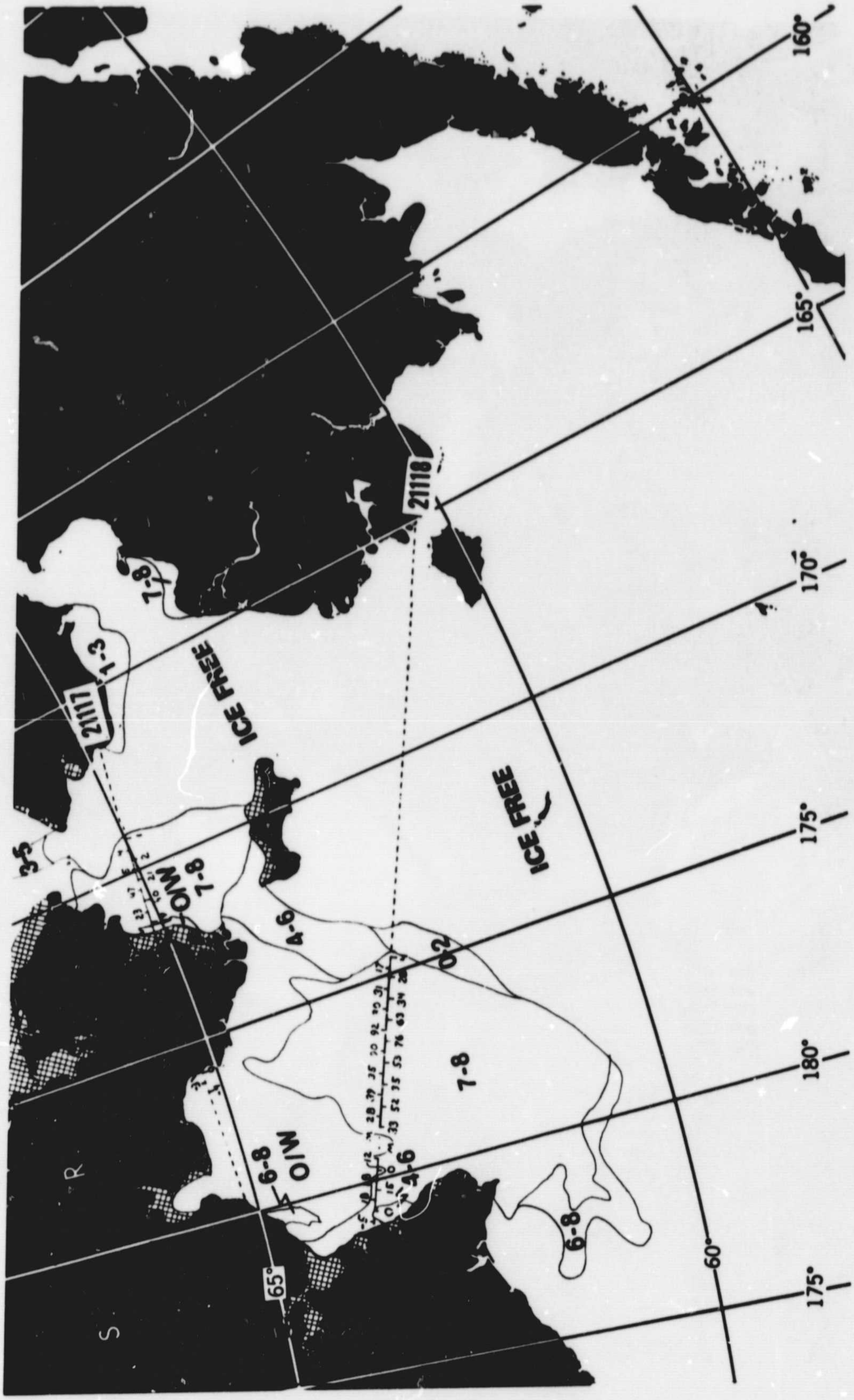

Fig. 5-7. Sea Ice Analysis May 11, 1979, with GEOS-3 Track 21117, 1338 GMT and Track 21118, 1518 GMT, May 11, 1979.

operational evaluations, the radar altimeter has demonstrated an ice detection capability. Its day/night all weather capability and relatively small footprint makes it a useful tool for accurately locating ice edge positions. Qualitatively, low positive index values correlate with lesser ice concentrations and with very rough higher ice concentrations. High index values appear to correlate best with smoother young ice. The altimeter also has demonstrated the capability of detecting open water bounded by ice packs.

References

1. Hofmeister, E.L., Keeney, B.N., Godbey, T.W., and Berg, R.J.: "Data Users Handbook and Design Error Analysis," GEOS-C Radar Altimeter, Volume I, General Electric Co., Utica, NY, May 1976.

2. Walsh, E.J., Uliana, E.A., Yaplee, B.S.: "Ocean Wave Heights Measured by a High Resolution Pulse-Limited Radar Altimeter," Boundary-Layer Meteorology, Volume 13, pp. 263-276, 1978.

3. GEOS-3 Project: "Geodynamics Experimental Ocean Satellite (GEOS-3) Near-Real-Time Significant Wave Height and Wind Speed Data Systems," NASA Wallops Flight Center, Wallops Island, VA, March 1978.

4. Fedor, L.S., Godbey, T.W., Gower, J.F.R., Guptill, R., Hayne, G.S., Rufenach, C.L., and Walsh, E.J.: "Satellite Altimeter Measurements of Sea State - An Algorithm Comparison," Journal of Geophysical Research, American Geophysical Union, Volume 84, Number B8, July 30, 1979.

5. Brown, G.S.: "Estimation of Surface Wind Speeds Using Satellite-Borne Radar Measurements at Normal Incidence," Journal of Geophysical Research, American Geophysical Union, Volume 84, Number B8, July 30, 1979.

6. Leitao, C.D., Huang, N.E., Parra, C.G.: "A Note on the Comparison of Radar Altimetry with IR and In Situ Data for the Detection of the Gulf Stream Surface Boundaries," Journal of Geophysical Research, American Geophysical Union, Volume 84, Number B8, July 30, 1979.

7. Fett, R.W., Mitchell, W.F.: "Navy Tactical Applications Guide, Volume 1, Techniques and Applications of Image Analysis," Naval Environmental Prediction Research Facility, Monteray, CA, January 1977.

8. Hussey, W.J.: "The TIROS-N Polar Orbiting Environmental Satellite System," National Environmental Satellite Service, NOAA, Washington, D.C., October 1977.

Appendix A

This appendix contains the set of GEOS-3 data files analysed in Section 5. The data include both the ice files and the associated surface wind speed file for each arc of data.

It should be noted that the latitude (lat) and longitude (long) columns of some of the ice files have been corrected after the fact to reflect more precise positions. In March 1979, the real-time system orbit generator was not accurate enough for the ice-edge discrimination application. This inadequacy was overcome by deriving accurate positions off-line and then phoning these results (altered positions in time) to the ice center. In April 1979, the real-time system inadequacy was completely overcome by establishing the precise orbit generator in the real-time-system itself.

The data files are organized with the wind data file first for each arc of data. The wind data file header record identifies the GEOS-3 satellite (GEOC), the orbit number and the date (YY/MM/DD). ASCTIM is the time of the ascending node (DD HH MM SS) and ASCLON is the east longitude of the ascending node in degrees used to calculate the orbital positions (and lat/long) for the arc of data. The header record for the ice file contains only the orbit number and date.

!LISM A20120

GEOC 20120 79/03/02 ASCTIM 61 2 9 31 ASCLON 323.32

TIME	LAT	LONG	H1/3	GAM	◆◆◆◆◆◆◆◆◆◆◆ W I N D S ◆◆◆◆◆◆◆◆◆◆◆				
23853	61.62	-164.31			3.4/2	3.4/3	3.5/3	2.4/3	12.1/2
240 9	59.33	-172.46			12.1/3	11.7/3	11.6/3	11.6/3	11.5/3
24029	58.66	-174.43			11.3/3	11.3/3	11.3/3	11.1/3	10.3/3
24050	57.92	-176.41			10.0/3	9.8/3	9.4/3	9.5/3	9.4/3
24110	57.19	-178.23			7.3/3	6.0/3	5.6/3	5.7/3	6.2/3
24131	56.40	179.94			6.1/3	5.8/3	6.2/3	5.8/3	4.9/3
24151	55.63	178.26			4.8/3	4.8/3	4.2/3	4.1/3	4.7/3
24212	54.80	176.56			5.7/3	6.4/3	7.0/3	4.5/3	3.4/3
24232	53.99	175.01			4.0/3	2.6/2	1.6/2	1.4/3	1.8/3
24259	52.86	173.00			2.9/3	4.6/3	3.3/2	3.4/3	3.1/3
24328	51.63	170.95			3.3/3	4.6/3	5.6/3	5.7/3	6.6/3
24348	50.75	169.59			7.3/3	8.9/3	9.6/3	10.0/3	10.7/3
244 9	49.82	168.22			11.2/3	11.5/3	11.7/3	11.9/3	11.8/3
24429	48.93	166.96			11.9/3	12.1/3	12.6/3	12.9/2	

!LIST ICE

ICE FILE - 20120 79/03/02

TIME	TCG	LAT.	LONG.	AASG	AGC	INDEX
23822	5465873	62.42	-160.67	.019	-76.757	2
23825	5465874	62.34	-161.03	.034	-74.224	-2
23827	5465875	62.29	-161.27	.035	-74.190	-2
23847	5465885	61.78	-163.62	.033	-72.581	-1
23849	5465886	61.73	-163.85	.034	-71.999	-1
23851	5465887	~~61.68~~	~~-164.08~~	.040	-71.953	-2
23912	5465897	61.35	-166.11	.020	-59.501	10
23914	5465898	61.29	-166.33	.010	-58.002	30
23916	5465899	61.23	-166.55	.007	-57.476	51
23918	5465900	61.18	-166.77	.007	-57.220	55
23920	5465901	61.12	-166.99	.005	-56.923	70
23922	5465902	61.06	-167.21	.006	-57.571	63
23924	5465903	61.00	-167.43	.007	-58.799	53
23926	5465904	60.94	-167.65	.007	-60.257	44
23928	5465905	60.88	-167.86	.008	-60.135	39
23930	5465906	60.83	-168.08	.010	-60.486	29
23932	5465907	60.77	-168.29	.009	-58.948	36
23934	5465908	60.71	-168.51	.008	-60.028	39
23936	5465909	60.65	-168.72	.009	-60.365	35
23938	5465910	60.59	-168.93	.009	-60.284	33
23940	5465911	60.52	-169.15	.008	-60.311	37
23942	5465912	60.46	-169.36	.011	-63.173	23
23944	5465913	60.40	-169.57	.012	-61.988	21
23946	5465914	60.34	-169.78	.009	-60.847	32
23948	5465915	60.28	-169.99	.012	-65.227	18
23951	5465916	60.19	-170.30	.013	-64.411	18
23953	5465917	60.12	-170.51	.016	-65.899	11
23955	5465918	60.06	-170.71	.017	-63.120	12
23957	5465919	60.00	-170.92	.017	-64.437	10
23959	5465920	59.93	-171.12	.024	-68.559	2
240 1	5465921	59.87	-171.33	.034	-71.265	-1
240 3	5465922	59.80	-171.53	.043	-74.450	-4

!LIST A20123

GEDC 20123 79/03/02 ASCTIM 61 7 14 50 ASCLON 247.36

TIME	LAT	LONG	H1/3	GAM	◆◆◆◆◆◆◆◆◆◆◆ W	I N D	S ◆◆◆◆◆◆◆◆◆◆◆		
729 8	44.39	-143.36			3.8/1	3.7/3	3.9/3	4.0/3	4.2/3
72931	45.48	-144.60			4.3/3	4.3/3	4.4/3	4.8/3	4.7/3
72951	46.42	-145.72			5.0/3	5.3/3	5.5/3	5.3/3	5.5/3
73012	47.39	-146.93			5.7/3	5.6/3	6.1/3	6.0/3	5.9/3
73032	48.31	-148.12			5.7/3	6.0/3	6.4/3	6.3/3	6.3/3
73053	49.26	-149.41			7.1/3	7.0/3	6.5/3	6.3/3	6.5/3
73113	50.16	-150.69			6.3/3	6.1/3	6.1/3	6.3/2	7.5/3
73138	51.25	-152.35			7.4/3	7.0/3	7.2/3	7.8/3	8.4/2
732 0	52.20	-153.87			8.9/3	8.5/3	8.8/3	8.9/3	9.0/3
73221	53.09	-155.38			8.4/2	6.7/3	5.5/3	4.9/3	4.9/3
73243	54.01	-157.03			4.7/3	5.5/3	7.8/3	9.9/3	10.4/3
733 4	54.86	-158.66			10.5/3	10.5/3	8.4/3	3.6/3	2.1/2
73337	56.15	-161.37			6.0/3	6.5/3	6.8/3	6.8/3	6.9/3
73357	56.91	-163.09			6.9/3	6.8/3	6.1/3	5.6/3	5.4/3
73417	57.65	-164.88			5.5/3	6.1/3	5.4/3	10.2/2	9.8/2
736 2	61.08	-175.47			4.9/3	10.5/3	11.0/3	10.7/3	10.8/3
73622	61.63	-177.73			10.5/3	10.3/3	10.6/3	10.8/3	10.8/3
73643	62.18	179.82			10.9/2	13.6/2	87.8/3		

!LIST ICE

ICE FILE - 20123 79/03/02

TIME	TCG	LAT.	LONG.	AASG	AGC	INDEX
73434	5474550	58.37	-166.33	.027	-65.632	2
73436	5474551	58.44	-166.51	.023	-65.946	5
73438	5474552	58.51	-166.70	.022	-64.745	6
73440	5474553	58.58	-166.89	.023	-64.692	5
73442	5474554	58.65	-167.08	.020	-63.687	8
73444	5474555	58.72	-167.27	.020	-62.773	8
73446	5474556	58.79	-167.46	.016	-62.668	13
73448	5474557	58.86	-167.66	.012	-62.668	20
73450	5474558	58.93	-167.85	.012	-65.319	19
73452	5474559	58.99	-168.04	.012	-65.554	19
73454	5474560	59.06	-168.24	.013	-65.502	15
73456	5474561	59.13	-168.43	.011	-62.720	22
73458	5474562	59.20	-168.63	.010	-62.276	29
735 0	5474563	59.26	-168.82	.011	-63.243	24
735 3	5474564	59.36	-169.12	.011	-62.015	24
735 5	5474565	59.43	-169.32	.013	-63.752	18
735 7	5474566	59.50	-169.52	.016	-63.373	12
735 9	5474567	59.56	-169.72	.012	-64.065	20
73511	5474568	59.63	-169.92	.014	-65.450	15
73513	5474569	59.69	-170.12	.015	-64.823	13
73515	5474570	59.76	-170.32	.014	-64.966	14
73517	5474571	59.82	-170.52	.019	-65.711	7
73519	5474572	59.88	-170.73	.018	-64.130	10
73521	5474573	59.95	-170.93	.017	-63.543	11
73523	5474574	60.01	-171.14	.016	-64.927	11
73525	5474575	60.08	-171.34	.023	-69.170	3
73527	5474576	60.14	-171.55	.030	-69.730	0
73529	5474577	60.20	-171.76	.035	-68.002	0
73531	5474578	60.26	-171.96	.019	-63.895	9
73533	5474579	60.33	-172.17	.017	-65.711	9
73535	5474580	60.39	-172.38	.013	-63.452	18
73537	5474581	60.45	-172.59	.013	-65.737	15
73539	5474582	60.51	-172.80	.025	-69.599	2
73541	5474583	60.57	-173.02	.028	-68.323	1
73543	5474584	60.63	-173.23	.022	-67.730	4
73546	5474585	60.72	-173.55	.025	-71.659	1
73548	5474586	60.78	-173.76	.039	-74.840	-3
73550	5474587	60.84	-173.98	.041	-74.942	-3
73647	5474615	62.39	179.56	.031	-68.764	0
73649	5474616	62.44	179.32	.025	-70.979	1
73651	5474617	62.49	179.09	.018	-74.726	4

!LIST A20137

GEOC 20137 79/03/03 ASCTIM 62 6 59 39 ASCLON 252.88

TIME	LAT	LONG	H1/3	GAM	◆◆◆◆◆◆◆◆◆◆◆ W	I N D S	◆◆◆◆◆◆◆◆◆◆◆		
7 749	25.89	-122.24			2.8/2	3.0/3	3.2/3	3.2/3	3.2/3
7 810	26.99	-122.98			3.4/3	3.4/3	3.2/3	3.1/3	3.3/3
7 830	28.02	-123.69			3.2/3	3.1/3	3.0/3	3.0/3	2.8/3
7 851	29.11	-124.46			2.6/3	2.7/3	2.5/3	2.2/3	2.0/3
7 911	30.14	-125.20			1.7/3	1.4/3	1.4/3	1.5/3	1.2/2
7 934	31.32	-126.07			1.0/2	1.1/3	1.2/3	1.1/2	1.5/3
7 958	32.55	-127.00			2.0/3	2.3/3	2.3/3	2.2/3	2.4/3
71019	33.62	-127.84			2.5/3	2.9/3	3.1/3	3.3/3	3.3/3
71039	34.64	-128.65			3.5/3	3.6/3	3.7/3	3.8/3	4.1/3
711 0	35.70	-129.52			3.9/3	3.7/3	3.7/3	3.8/3	3.9/3
71120	36.70	-130.37			4.0/3	4.0/3	3.9/3	4.1/3	4.3/3
71141	37.75	-131.28			4.2/3	4.2/3	4.4/3	4.3/3	4.3/3
712 1	38.75	-132.17			4.2/3	4.3/3	4.6/3	4.7/3	5.0/3
71222	39.79	-133.14			5.4/3	5.7/3	5.5/3	5.2/3	4.9/3
71242	40.77	-134.08			5.1/3	5.2/3	4.8/3	4.6/3	4.5/3
713 3	41.80	-135.09			4.7/3	4.4/3	4.4/3	4.7/3	4.7/3
71323	42.76	-136.09			4.6/3	4.6/3	4.5/3	4.4/3	4.5/3
71350	44.06	-137.47			4.0/2	3.9/3	3.8/3	3.9/3	4.2/3
71410	45.01	-138.54			4.1/3	4.3/3	4.3/3	4.4/3	4.5/3
71431	46.00	-139.69			4.5/3	4.4/3	4.5/3	4.6/3	4.6/3
71451	46.93	-140.83			4.7/3	5.1/3	4.8/3	4.7/3	4.9/3
71512	47.90	-142.06			4.5/3	4.8/3	4.8/3	4.7/3	4.8/3
71532	48.81	-143.27			4.9/3	4.8/3	4.8/3	4.9/3	5.2/3
71553	49.76	-144.59			4.6/3	4.6/3	5.1/3	5.3/3	5.5/3
71613	50.64	-145.89			5.3/3	5.3/3	5.8/3	6.0/3	6.1/3
71634	51.56	-147.31			6.4/3	6.3/3	6.1/3	6.3/3	6.8/3
71654	52.42	-148.70			6.8/3	7.2/3	6.8/3	6.8/3	6.2/3
71715	53.30	-150.23			6.1/3	6.6/3	5.4/3	4.5/3	3.8/3
71735	54.13	-151.74			2.7/3	2.1/3	2.9/3	4.2/3	4.2/3
71756	54.98	-153.38			3.7/3	2.6/3	[illegible]	3.8/3	3.9/3
71816	55.77	-155.01			3.2/3	3.8/3	[illegible]	3.7/3	2.8/3
71839	56.65	-156.96			1.2/1	3.6/2	5.4/2	6.6/3	10.4/3
72246	63.76	176.06			13.6/3	13.1/2			

!LIST ICE

ICE FILE - 20137 79/03/03

TIME	TCG	LAT.	LONG.	AASG	AGC	INDEX
71849	5516274	57.15	-157.72	.028	-73.106	0
71851	5516275	57.22	-157.90	.027	-67.481	1
71853	5516276	57.30	-158.07	.025	-69.494	2
71855	5516277	57.37	-158.25	.040	-73.174	-3
71857	5516278	57.44	-158.43	.045	-73.448	-4
719 3	5516281	57.66	-158.97	.022	-64.147	6
719 5	5516282	57.73	-159.15	.015	-63.568	14
719 7	5516283	57.81	-159.33	.015	-63.924	14
719 9	5516284	57.88	-159.51	.016	-64.437	11
71911	5516285	57.95	-159.69	.014	-62.659	16
71913	5516286	58.02	-159.88	.016	-62.738	13
71916	5516287	58.13	-160.15	.011	-59.798	27
71918	5516288	58.20	-160.34	.010	-59.285	32
71920	5516289	58.27	-160.53	.009	-57.732	38
71922	5516290	58.34	-160.71	.007	-57.152	52
71924	5516291	58.41	-160.90	.008	-56.625	46
71926	5516292	58.48	-161.09	.004	-54.825	106
71928	5516293	58.55	-161.28	.003	-54.968	118
71930	5516294	58.62	-161.47	.019	-70.772	5
71932	5516295	58.69	-161.66	.034	-64.279	0
71934	5516296	58.76	-161.85	.009	-58.057	35
71936	5516297	58.82	-162.04	.007	-58.448	53
71938	5516298	58.89	-162.23	.007	-59.096	52
71940	5516299	58.96	-162.43	.008	-59.245	43
71942	5516300	59.03	-162.62	.007	-58.880	49
71944	5516301	59.10	-162.81	.007	-59.582	48
71946	5516302	59.16	-163.01	.007	-60.847	50
71948	5516303	59.23	-163.21	.007	-60.271	51
71950	5516304	59.30	-163.40	.008	-61.290	40
71952	5516305	59.36	-163.60	.007	-59.960	48
71954	5516306	59.43	-163.80	.006	-57.463	63
71956	5516307	59.50	-164.00	.005	-57.908	74
71959	5516308	59.59	-164.30	.007	-58.002	54
720 1	5516309	59.66	-164.50	.007	-58.354	54
720 3	5516310	59.72	-164.70	.008	-60.176	39
720 5	5516311	59.79	-164.90	.010	-61.082	27
720 7	5516312	59.85	-165.11	.010	-60.189	30
720 9	5516313	59.92	-165.31	.012	-64.938	19
72011	5516314	59.98	-165.51	.032	-73.363	-1
72013	5516315	60.04	-165.72	.043	-75.367	-4
72015	5516316	60.11	-165.93	.036	-73.099	-2
72023	5516320	60.36	-166.76	.013	-60.135	21
72025	5516321	60.42	-166.97	.010	-60.999	29
72027	5516322	60.48	-167.18	.010	-59.231	32
72029	5516323	60.54	-167.39	.007	-58.381	50
72031	5516324	60.60	-167.60	.007	-58.637	53
72033	5516325	60.66	-167.82	.006	-58.340	62
72035	5516326	60.72	-168.03	.007	-59.164	52
72037	5516327	60.78	-168.24	.008	-59.298	40
72039	5516328	60.84	-168.46	.008	-60.135	39

Ice File 20137 (continued)

72042	5516329	60.93	-168.78	.011	-61.566	26
72044	5516330	60.99	-169.00	.011	-59.663	26
72046	5516331	61.05	-169.22	.008	-59.811	37
72048	5516332	61.10	-169.44	.010	-60.735	31
72050	5516333	61.16	-169.66	.008	-60.597	37
72052	5516334	61.22	-169.88	.008	-59.811	42
72054	5516335	61.28	-170.10	.007	-60.763	44
72056	5516336	61.33	-170.32	.008	-60.230	39
72058	5516337	61.39	-170.54	.008	-61.026	36
721 0	5516338	61.44	-170.77	.011	-61.619	23
721 2	5516339	61.50	-170.99	.009	-59.777	35
721 4	5516340	61.56	-171.21	.008	-59.804	42
721 6	5516341	61.61	-171.44	.009	-60.536	35
721 8	5516342	61.67	-171.67	.009	-59.737	35
72110	5516343	61.72	-171.89	.007	-58.697	46
72112	5516344	61.77	-172.12	.006	-59.574	52
72114	5516345	61.83	-172.35	.007	-59.642	45
72116	5516346	61.88	-172.58	.008	-62.471	34
72118	5516347	61.93	-172.81	.012	-65.433	18
72120	5516348	61.99	-173.04	.011	-64.058	23
72122	5516349	62.04	-173.27	.009	-65.486	29
72125	5516350	62.11	-173.62	.010	-65.684	26
72127	5516351	62.17	-173.86	.011	-67.078	20
72129	5516352	62.22	-174.09	.014	-64.547	14
72131	5516353	62.27	-174.33	.012	-64.257	19
72133	5516354	62.32	-174.56	.012	-62.590	20
72135	5516355	62.37	-174.80	.012	-65.486	18
72137	5516356	62.42	-175.04	.013	-63.489	18
72139	5516357	62.47	-175.27	.013	-63.238	18
72141	5516358	62.51	-175.51	.009	-60.425	33
72143	5516359	62.56	-175.75	.008	-62.299	34
72145	5516360	62.61	-175.99	.011	-63.251	24
72147	5516361	62.66	-176.24	.013	-63.119	19
72149	5516362	62.70	-176.48	.013	-63.423	18
72151	5516363	62.75	-176.72	.012	-61.664	21
72153	5516364	62.80	-176.96	.010	-63.066	25
72155	5516365	62.84	-177.21	.014	-64.600	14
72157	5516366	62.89	-177.45	.013	-65.486	15
72159	5516367	62.93	-177.70	.017	-66.107	9
722 1	5516368	62.98	-177.94	.017	-66.081	9
722 3	5516369	63.02	-178.19	.020	-64.970	7
722 6	5516370	63.09	-178.56	.015	-65.089	13
722 8	5516371	63.13	-178.81	.017	-65.949	9
72210	5516372	63.17	-179.06	.016	-66.430	10
72212	5516373	63.22	-179.31	.019	-67.165	7
72214	5516374	63.26	-179.56	.010	-62.511	26
72216	5516375	63.30	-179.81	.011	-66.243	19
72218	5516376	63.34	179.93	.017	-71.851	6
72220	5516377	63.38	179.68	.014	-71.967	9
72222	5516378	63.42	179.43	.015	-71.676	8
72224	5516379	63.46	179.17	.015	-68.248	10
72226	5516380	63.50	178.92	.030	-74.220	-1
72228	5516381	63.54	178.66	.048	-73.277	-4
72230	5516382	63.58	178.40	.051	-75.346	-5

GEOC 20478 79/03/27 086 09 23 46 258.78 (VER.5)

TIME	LAT	LONG	H1/3	GAM	W	I	N	D	S
93139	25.11	-115.80			2.2/1	2.2/3	2.2/3	2.2/3	2.2/3
932 6	26.52	-116.75			2.2/3	2.2/2	2.3/3	2.3/3	2.5/3
93229	27.71	-117.57			2.6/3	2.8/3	3.0/3	3.1/3	3.4/3
93249	28.75	-118.29			3.8/3	4.1/3	4.3/3	4.2/3	4.3/3
93310	29.83	-119.07			4.3/3	4.1/3	4.3/3	4.6/3	5.1/3
93330	30.86	-119.82			5.5/3	6.6/3	8.6/3	8.0/3	7.6/3
93350	31.89	-120.59			7.5/3	7.7/3	9.2/3	9.3/3	8.0/3
93411	32.96	-121.41			6.2/3	5.8/3	5.4/3	5.9/3	6.7/3
93431	33.98	-122.21			7.0/3	8.1/3	8.8/3	9.3/3	9.7/3
93452	35.04	-123.07			9.9/3	10.0/3	9.9/3	9.9/3	10.1/3
93512	36.05	-123.91			10.5/3	10.8/3	10.7/3	11.1/3	10.8/3
93533	37.10	-124.80			10.9/3	11.2/3	10.4/3	9.4/3	8.3/3
93553	38.10	-125.68			8.3/3	7.0/3	5.6/3	5.3/3	5.0/3
93614	39.15	-126.63			4.7/3	4.2/3	5.9/3	7.6/3	7.9/3
93634	40.13	-127.55			10.1/3	11.6/3	12.0/3	12.0/3	11.4/3
93655	41.16	-128.55			10.8/3	11.0/3	11.1/3	10.5/3	10.2/3
93715	42.14	-129.53			10.0/3	9.7/3	9.6/3	9.5/3	9.6/2
93740	43.34	-130.79			9.6/3	9.5/3	9.4/3	9.3/3	9.6/3
938 0	44.30	-131.83			9.7/3	10.0/3	10.2/3	10.0/3	9.9/3
93821	45.29	-132.95			10.0/3	10.3/3	10.9/3	9.8/1	9.8/3
93856	46.93	-134.92			9.7/2	9.2/3	8.6/3	8.2/3	8.8/3
93926	48.31	-136.69			8.4/3	7.2/2	7.2/3	7.1/3	6.8/3
93951	49.44	-138.23			6.5/3	6.6/3	6.7/3	6.6/3	7.0/3
94011	50.33	-139.52			7.0/3	6.8/3	6.3/3	5.9/3	5.6/3
94032	51.25	-140.92			5.5/3	5.5/3	5.5/3	5.3/3	5.2/3
94052	52.12	-142.30			5.1/3	4.9/3	5.2/3	5.3/3	5.1/3
94113	53.01	-143.80			5.2/3	5.3/3	6.1/3	5.8/3	5.6/3
94133	53.84	-145.29			6.0/3	6.5/3	7.1/3	7.7/3	7.8/3
94154	54.70	-146.92			8.3/3	8.6/3	9.3/3	9.6/3	9.3/2
94216	55.57	-148.69			9.3/3	9.4/3	9.4/3	8.2/3	6.7/3
94237	56.38	-150.45			6.3/3	6.1/3	5.3/3	5.3/3	6.0/3
94257	57.14	-152.19			6.4/3	3.7/1	9.5/3	12.8/2	0. /1

ICE FILE - 20478 79/03/27

TIME	TCG	LAT.	LONG.	AASG	AGC	JEX
94512	6533012	61.58	-165.64	.022	-70.837	3
94515	6533013	61.66	-165.98	.025	-70.760	1
94517	6533014	61.71	-166.21	.042	-72.043	-3
94521	6533016	61.82	-166.67	.025	-67.258	3
94523	6533017	61.87	-166.90	.014	-63.748	15
94525	6533018	61.92	-167.13	.019	-64.698	8
94527	6533019	61.98	-167.36	.016	-65.014	12
94529	6533020	62.03	-167.59	.018	-67.872	7
94533	6533022	62.13	-168.05	.015	-67.565	11
94535	6533023	62.18	-168.29	.015	-66.426	12
94537	6533024	62.23	-168.53	.010	-63.376	25
94539	6533025	62.28	-168.76	.008	-62.399	39
94541	6533026	62.33	-169.00	.007	-61.875	45
94543	6533027	62.38	-169.23	.010	-63.624	26
94545	6533028	62.43	-169.47	.009	-63.486	31
94547	6533029	62.48	-169.71	.012	-65.439	18
94549	6533030	62.52	-169.94	.012	-64.491	19

Ice File 20478 (continued)

94551	6533031	62.57	-170.19	.009	-63.073	30
94553	6533032	62.62	-170.43	.007	-62.096	45
94555	6533033	62.67	-170.67	.014	-68.620	11
94558	6533034	62.74	-171.04	.035	-71.482	-1
946 0	6533035	62.78	-171.28	.033	-70.862	-1
946 2	6533036	62.83	-171.53	.033	-70.596	-1
946 4	6533037	62.88	-171.77	.039	-69.899	-2
946 8	6533039	62.97	-172.26	.017	-65.542	9
94610	6533040	63.01	-172.51	.010	-64.229	25
94612	6533041	63.06	-172.76	.016	-66.988	11
94614	6533042	63.10	-173.01	.014	-64.628	15
94618	6533044	63.19	-173.52	.017	-67.514	9
94620	6533045	63.23	-173.77	.023	-71.662	2
94622	6533046	63.27	-174.02	.016	-62.605	14
94624	6533047	63.31	-174.28	.010	-63.486	27
94626	6533048	63.35	-174.53	.014	-64.051	16
94628	6533049	63.38	-174.80	.011	-63.996	23
94632	6533051	63.47	-175.31	.006	-61.959	56
94634	6533052	63.51	-175.57	.006	-63.093	54
94636	6533053	63.55	-175.83	.007	-67.259	38
94639	6533054	63.60	-176.22	.008	-65.525	31
94641	6533055	63.64	-176.48	.011	-64.861	23
94643	6533056	63.68	-176.74	.006	-64.019	45
94645	6533057	63.71	-177.00	.008	-66.373	30
94647	6533058	63.75	-177.26	.006	-64.475	45
94651	6533060	63.82	-177.79	.009	-73.234	18
94653	6533061	63.85	-178.06	.010	-69.796	19
94655	6533062	63.89	-178.32	.007	-64.682	41
94657	6533063	63.92	-178.59	.008	-67.708	28
94659	6533064	63.95	-178.85	.006	-62.789	47
947 1	6533065	63.99	-179.12	.010	-72.048	17
947 3	6533066	64.02	-179.40	.011	-70.750	17
947 5	6533067	64.05	-179.66	.007	-66.578	39
947 7	6533068	64.08	-179.93	.009	-71.677	19
947 9	6533069	64.11	179.80	.009	-67.760	24
94713	6533071	64.17	179.26	.005	-66.681	52
94715	6533072	64.20	178.99	.009	-68.104	23
94717	6533073	64.23	178.72	.021	-75.282	1
94719	6533074	64.26	178.45	.034	-75.474	-2
94724	6533076	64.33	177.77	.040	-74.240	-3
94726	6533077	64.36	177.49	.036	-73.917	-2
94746	6533087	64.60	174.73	.029	-73.665	-1
94750	6533089	64.64	174.18	.034	-76.017	-2
94752	6533090	64.66	173.90	.057	-78.720	-6

GEOC 21117 79/05/11 131 13 14 04 279.84 (VER.5)

TIME	LAT	LONG	H1/3	GAM	WINDS				
133826.0	64.85	-166.83			4.0/2	4.9/3	6.2/3	6.9/3	
133936.0	65.15	-176.79			10.1/2	9.3/3	7.0/3	6.5/3	7.2/3
133956.0	65.12	-179.66			5.3/2				
1340 4.0	65.09	179.20			19.9/1				
134029.0	64.95	175.65			31.5/2	20.9/3			
134049.0	64.79	172.84			0. /1				

ICE FILE - 21117 79/05/11

TIME	TCG	LAT.	LONG.	AASG	AGC	INDEX
133818.0	8438183	64.78	-165.71	.094	-88.899	-8
133820.0	8438184	64.80	-165.99	.114	-90.610	-9
133822.0	8438185	64.82	-166.27	.129	-79.936	-8
133824.0	8438186	64.83	-166.55	.063	-69.116	-5
133842.0	8438195	64.97	-169.08	.026	-70.769	1
133845.0	8438196	64.99	-169.51	.019	-72.368	4
133847.0	8438197	65.01	-169.79	.022	-72.854	2
133849.0	8438198	65.02	-170.07	.020	-69.189	5
133851.0	8438199	65.03	-170.36	.012	-62.238	21
133853.0	8438200	65.04	-170.64	.007	-60.843	47
133855.0	8438201	65.05	-170.93	.007	-63.619	40
133857.0	8438202	65.06	-171.21	.011	-64.679	23
133859.0	8438203	65.07	-171.50	.011	-67.532	19
1339 1.0	8438204	65.08	-171.78	.028	-68.965	1
1339 3.0	8438205	65.09	-172.07	.020	-64.826	7
1339 9.0	8438208	65.11	-172.92	.053	-88.378	-7
133915.0	8438211	65.12	-173.78	.028	-81.262	-3
133921.0	8438214	65.14	-174.64	.035	-82.887	-5
133928.0	8438217	65.14	-175.64	.036	-76.757	-3
133930.0	8438218	65.15	-175.93	.025	-72.986	0
133932.0	8438219	65.15	-176.22	.037	-74.358	-3
133934.0	8438220	65.15	-176.50	.043	-74.699	-4
133958.0	8438232	65.11	-179.94	.026	-74.201	0
1340 0.0	8438233	65.10	179.77	.039	-77.276	-4
1340 2.0	8438234	65.10	179.49	.057	-77.833	-6
1340 6.0	8438236	65.08	178.92	.031	-79.076	-3
1340 8.0	8438237	65.07	178.63	.048	-79.403	-5
134011.0	8438238	65.06	178.20	.032	-74.010	-1
134013.0	8438239	65.05	177.92	.027	-73.695	0
134015.0	8438240	65.04	177.63	.038	-75.433	-3
134017.0	8438241	65.03	177.35	.040	-76.589	-4
134019.0	8438242	65.02	177.07	.030	-76.173	-2
134021.0	8438243	65.01	176.78	.033	-76.089	-2
134023.0	8438244	64.99	176.50	.032	-76.958	-2
134025.0	8438245	64.98	176.22	.054	-81.635	-6
134027.0	8438246	64.97	175.93	.057	-80.093	-6
134037.0	8438251	64.89	174.52	.033	-76.644	-3
134039.0	8438252	64.88	174.24	.030	-75.703	-1
134041.0	8438253	64.86	173.96	.024	-74.352	0
134043.0	8438254	64.84	173.68	.036	-78.092	-3
134045.0	8438255	64.82	173.40	.037	-79.212	-4
134047.0	8438256	64.81	173.12	.051	-83.266	-6
134052.0	8438258	64.76	172.42	.059	-87.026	-7

GEOC 21118 79/05/11 131 14 55 51 254.52 (VER.5)

TIME	LAT	LONG	H1/3	GAM	◆◆◆◆◆◆◆◆◆◆◆ W	I N	D S	◆◆◆◆◆◆◆◆◆◆◆◆	
151150.0	49.21	-141.93			4.9/2	5.5/3	6.0/3	6.5/3	6.9/3
151210.0	50.11	-143.19			7.6/3	8.4/3	9.3/3	9.3/3	~~8.2/3~~
151231.0	51.03	-144.56			8.7/3	8.2/3	7.2/3	7.2/3	7.0/3
151251.0	51.90	-145.91			7.6/3	7.5/3	7.2/3	6.5/3	6.4/3
151312.0	52.79	-147.39			6.5/3	5.7/3	5.8/3	6.5/3	6.8/3
151332.0	53.63	-148.85			7.2/3	6.6/3	5.5/3	5.0/3	5.4/3
151353.0	54.49	-150.43			5.1/3	4.7/3	4.8/3	4.8/3	4.6/3
151413.0	55.29	-152.01			5.4/3	6.0/3	6.3/3	6.1/3	6.2/3
151434.0	56.11	-153.72			6.3/3	5.9/3	5.2/2		
151446.0	56.56	-154.74			4.6/2	4.4/3	4.8/3	5.6/3	5.3/2
151525.0	58.00	-158.19			6.6/2	7.1/3	7.3/3	5.9/3	5.8/3
151545.0	58.70	-160.06			6.2/2				
151549.0	58.84	-160.44			7.3/1				
151610.0	59.54	-162.50			3.0/2	~~2.4/3~~			
151647.0	60.70	-166.33			1.0/2	1.4/3	2.6/3	3.3/3	4.1/3
1517 7.0	61.29	-168.50			4.1/3	4.1/3	4.4/3	4.9/3	5.4/3
151728.0	61.86	-170.87			5.4/3	5.5/3	5.8/3	5.3/3	5.0/3
151748.0	62.38	-173.20			4.1/3	3.5/3	4.1/3		
1519 0.	63.90	177.79			17.0/2				
151912.0	64.10	176.21			22.9/2				

ICE FILE - 21118 79/05/11

TIME	TCG	LAT.	LONG.	AASG	AGC	INDEX
151144.0	8440920	48.94	-141.56	.026	-72.733	0
151146.0	8440921	49.03	-141.68	.041	-72.632	-3
151148.0	8440922	49.12	-141.80	.045	-72.790	-3
151444.0	8441008	56.49	-154.56	.033	-69.526	0
1515 4.0	8441018	57.24	-156.30	.022	-67.333	4
151512.0	8441022	57.53	-157.01	.011	-65.298	22
151515.0	8441023	57.64	-157.28	.009	-66.036	27
151519.0	8441025	57.79	-157.64	.024	-71.355	1
151521.0	8441026	57.86	-157.82	.041	-73.429	-3
151523.0	8441027	57.93	-158.00	.043	-73.632	-3
151551.0	8441041	58.91	-160.63	.032	-71.154	-1
151553.0	8441042	58.97	-160.83	.033	-79.293	-3
151555.0	8441043	59.04	-161.02	.066	-74.763	-6
151558.0	8441044	59.14	-161.31	.017	-64.857	11
1516 0.0	8441045	59.21	-161.51	.034	-77.625	-3
1516 4.0	8441047	59.34	-161.90	.031	-69.539	0
1516 6.0	8441048	59.41	-162.10	.042	-71.705	-3
1516 8.0	8441049	59.48	-162.30	.044	-71.574	-3
151618.0	8441054	59.80	-163.30	.015	-57.478	18
151620.0	8441055	59.87	-163.51	.011	-61.249	24
151622.0	8441056	59.93	-163.71	.005	-58.964	73
151624.0	8441057	59.99	-163.92	.004	-56.604	104
151626.0	8441058	60.06	-164.12	.008	-62.071	37
151628.0	8441059	60.12	-164.33	.009	-56.487	37
151630.0	8441060	60.18	-164.54	.005	-55.106	88
151632.0	8441061	60.24	-164.74	.005	-56.094	86
151634.0	8441062	60.31	-164.95	.013	-59.436	21
151636.0	8441063	60.37	-165.16	.017	-59.040	14
151638.0	8441064	60.43	-165.37	.023	-60.258	7
151641.0	8441065	60.52	-165.69	.031	-62.528	1
151643.0	8441066	60.58	-165.90	.038	-62.880	0
151645.0	8441067	60.64	-166.11	.039	-64.193	0

Ice File 21118 (continued)

1518 0.0	8441104	62.67	-174.64	.024	-64.371	4
1518 2.0	8441105	62.71	-174.88	.013	-64.682	17
1518 4.0	8441106	62.76	-175.12	.009	-64.948	28
1518 7.0	8441107	62.83	-175.49	.008	-65.482	31
1518 9.0	8441108	62.87	-175.73	.008	-65.008	34
151811.0	8441109	62.92	-175.98	.009	-63.127	30
151813.0	8441110	62.96	-176.23	.005	-61.202	63
151815.0	8441111	63.01	-176.47	.003	-65.127	92
151817.0	8441112	63.05	-176.72	.004	-64.059	76
151819.0	8441113	63.10	-176.97	.004	-62.086	90
151821.0	8441114	63.14	-177.22	.005	-67.227	53
151825.0	8441116	63.22	-177.72	.007	-67.379	35
151827.0	8441117	63.27	-177.97	.007	-68.991	35
151829.0	8441118	63.31	-178.22	.007	-66.342	39
151831.0	8441119	63.35	-178.47	.005	-66.786	52
151833.0	8441120	63.39	-178.73	.008	-69.464	28
151835.0	8441121	63.43	-178.98	.008	-66.905	33
151841.0	8441124	63.55	-179.74	.014	-68.880	12
151843.0	8441125	63.59	180.00	.030	-68.814	0
151845.0	8441126	63.62	179.74	.013	-63.218	18
151848.0	8441127	63.68	179.35	.013	-65.867	15
151850.0	8441128	63.72	179.10	.012	-66.490	18
151852.0	8441129	63.75	178.84	.024	-76.850	0
151854.0	8441130	63.79	178.58	.048	-79.412	-5
151856.0	8441131	63.83	178.32	.054	-79.016	-6
1519 4.0	8441135	63.96	177.27	.039	-77.240	-4
1519 8.0	8441137	64.03	176.74	.040	-78.196	-4
151910.0	8441138	64.06	176.47	.043	-78.071	-4
151916.0	8441141	64.16	175.67	.042	-80.628	-5
151918.0	8441142	64.19	175.41	.051	-93.718	-8
151926.0	8441146	64.31	174.33	.033	-74.999	-2
151928.0	8441147	64.34	174.06	.035	-76.070	-3
151931.0	8441148	64.38	173.65	.036	-76.807	-3
151933.0	8441149	64.41	173.38	.043	-80.955	-5
151941.0	8441153	64.51	172.29	.032	-79.262	-3